arXiv:1601.06544v1 [math.NA] 25 Jan 2016

Goal-oriented a posteriori error control for nonstationary convection-dominated transport problems

K. Schwegler, M. Bause*

Helmut Schmidt University, Faculty of Mechanical Engineering,
Holstenhofweg 85, 220433 Hamburg, Germany

Abstract. The numerical approximation of convection-dominated problems continues to remain subject of strong interest. Families of stabilization techniques for finite element methods were developed in the past. Adaptive techniques based on a posteriori error estimates offer potential for further improvements. However, there is still a lack in robust a posteriori error estimates in natural norms of the discretizations. Here we combine the dual weighted residual method for goal-oriented error control with stabilized finite element approximations. By a duality argument an error representation is derived on that a space-time adaptive approach is built. It differs from former works on the dual weighted residual method. Numerical experiments illustrate that our schemes are capable to resolve layers and sharp fronts with high accuracy and to further reduce spurious oscillations of approximations.

Keywords: Convection-dominated problems, stabilized finite element methods, goal-oriented a posteriori error control, dual weighted residual method, duality techniques

1. Introduction

In the last decades, since the pioneering works of the 1980's (cf., e.g., [29]), strong efforts were made in the development of accurate and efficient approximation schemes for convection-dominated flow and transport problems. For a review of fundamental concepts related to their analysis and approximation and a presentation of prominent robust numerical methods we refer to the monograph [44]. Convection-dominated

*bause@hsu-hh.de (corresponding author)

problems are of high practical interest. They arise in many branches of technology and, therefore, deservedly attracted substantial analysis. Applications can be found in fluid dynamics including turbulence modeling, electro-magnetism, semi-conductor devices, environmental and civil engineering as well as in chemical and biological scienes. If transport mechanisms are convection-dominated, solution profiles with sharp moving fronts, interior or boundary layers with complicated structures where important physical and chemical phenomena take place may occur. The development of numerical methods with the ability to capture the strong gradients of the exact solution without producing spurious oscillations or smearing effects continues to remain a challenging task.

In the recent years a substantial progress has been made in the numerical approximation of convection-dominated problems, even though a real breakthrough is still missing. Numerous families of stabilization concepts were proposed and studied for various discretization techniques; cf. [44]. Here we focus on finite element discretizations along with residual-based stabilizations. In particular, we use the streamline upwind Petrov–Galerkin (SUPG) method for our unsteady computations. For steady problems an additional shock-capturing stabilization is applied to further enhance the effect of the numerical method that is proposed in this work. Restricting ourselves to steady problems in some of our numerical experiments is done for the sake of simplicity. It is sufficient for illustrating the method's features we would like to investigate. In the literature shock-capturing stabilization is also often refered to as a spurious oscillations at layers diminishing (SOLD) method. The SUPG method reduces non-physical osciallations in streamline direction, whereas SOLD methods yield an additional stabilization in crosswind direction. For a review of prominent variants of SOLD methods and a competitive numerical investigation of the performance properties of SUPG and families of SOLD stabilizations we refer to, e.g., [33]. Besides the class of these residual-based stabilization techniques, flux-corrected transport schemes are further addressed in [33]. These techniques aim at a stabilization on the algebraic level; cf. [36]. In many works of the literature authors conclude that spurious osciallations in the numerical approximation of convection-dominated problems can be reduced by state-of-the-art stabilization techniques (cf., e.g., [8]), but nevertheless the results are not satisfactory yet (cf. [33]), in particular, if applications of practical interest and in three space dimensions are considered.

Adaptive mesh generation based on an a posteriori error control is nowadays a well known technique to capture singular phenomena and sharp gradients of solutions to partial differential equations in numerical simulations. For a review of a posteriori error estimation techniques for finite element methods and automatic mesh generation we refer, for instance, to the monograph [51]. Even though interior and boundary layers that arise in applications of practical interest cannot be resolved completely by adaptive finite element meshes, at least in a reasonable computing time, a further improvement and gain in accuracy may nevertheless be expected by applying the concepts of automatic mesh generation to stabilized finite element approximations of convection-dominated problems. However, the design of an adaptive method requires the provision of an appropriate a posteriori error estimator. The derivation such an

error estimator for convection-dominated problems, that is robust with respect to the small perturbation parameter of the partial differential equation, is delicious and has borne out to be a considerable source of trouble. So far, the quality of adaptively refined grids is often not satisfactory yet. Further, only a few contributions have been published yet for convection-dominated problems and the considered type of discretizations. This observation even holds for stationary problems. For a deeper discussion and further references we refer to [32] for the stationary case and to [17, 23] for evolutionary problems. Usually, existing a posteriori error analyses for convection-dominated problems are either not robust with respect to the small perturbation parameter, embodyed by increasing bounds for a vanishing perturbation parameter, or the a posteriori error estimates are not based on the natural norm of the discretization for that an a priori error analysis becomes feasible. For the stationary case, in [48] an a posteriori error bound is presented in the norm $(\|v\|_{\mathcal{L}^2(\Omega)} + \varepsilon^{1/2}\|\nabla v\|_{\mathcal{L}^2(\Omega)})^{1/2}$ with ε being the small diffusion parameter. The bound is not robust in ε. On the other hand, in [49] the dual norm of the convective derivative is added to the energy norm to get a robust error estimate with respect to the small diffusion parameter. An extension of this approach to evolutionary problems is given in [50]. For evolutionary problems more recent robust a posteriori estimators measuring the error in a space-time mesh-dependent dual norm can be found in [17]. They are based on a space-time equilibrated flux reconstruction and are locally computable. The estimator by itself is local-in-time and local-in-space and does not depend on dual norms. However, dual error norms are usually beyond a reasonable physical interpretation and hard to compute such that they are of little interest in applications and difficult to use in studies of the experimental order of convergence.

In [32] a robust residual-based a posteriori error estimate in the SUPG norm is presented for stationary convection-diffusion equations. Its derivation uses variational multiscale theory. Upper and lower bounds are provided where the global upper bound relies on some hypotheses. A similar situation can be found in [14]. In [32] it is argumed and demonstrated by numerical experiments that the hypotheses are fulfilled and non restrictive in standard applications. The a priori error estimate in [32] is based on different weights than other residual-based error estimators for convection-diffusion-reaction problems. However it is noted that the estimator performs well if the solution posses only one kind of singularity. Otherwise the non-robust residual-based estimator for the $\mathcal{L}^2(\Omega)$ norm should be prefered. In [23] an adaptive SUPG method is proposed for time-dependent convection-diffusion problems where the SUPG solution is considered as a solution of a steady-state problem such that the error estimator of [32] becomes applicable. However, the approach relies on the heuristic argument that a certain term is of higher order and thus becomes negligible. A validation of the assumption is given for one space dimension. In numerical calculations the robustness of the error estimator and its superiority over the adaptive approach that is presented in [21] and built upon heuristic error indicators is illustrated. A further non-robust a posteriori error of residual type estimator is presented in [2]. Finally, we note that a posteriori error estimates are available for space-time finite element methods, cf. e.g. [39], and for Lagrange–Galerkin methods, cf. [10, 28], that are based on the method

of characteristics and represent another class of prominent schemes for the approximation of evolutionary convection-dominated problems (cf. [27]). A robust a priori error estimate for the Lagrange–Galerkin method with error constants depending only on norms of the data and not on (higher order) norms of the solution is presented in [5]. The estimate is proved in a Lagrangian framework instead of using Eulerian coordinates as it is done in most of the error analyses for Lagrange-Galerkin methods.

The dual weighted residual method (or shortly DWR method) [3] aims at the economical computation of arbitrary quantities of physical interest by properly adapting the computational mesh. Thus, the mesh adaption is based on the computation and control of a physically relevant goal quantity instead of the traditional energy-norm or the $\mathcal{L}^2$-norm. The DWR approach relies on a space-time variational formulation of the discrete problem and uses duality techniques to find a rigorous a posteriori error estimate. Such duality techniques are well known from a prior error analyses; cf., e.g., [18, 19, 26]. The DWR approach has been applied to the numerical approximation of several classes of mathematical models based on partial differential equations, including fluid mechanics [13], wave propagation [4], structural mechanics [41], fluid-structure interaction [42], eigenvalue problems [25], optimization problems [38] and, further, been applied to goal-oriented adaptive modeling [12]. In the abstract DWR philosophy (cf. [3] for details) an error representation for the considered goal quantity is derived by dualityx techniques at the beginning. This error identity cannot be evaluated directly, since it depends on the unknown solution of the "linearized" dual or adjoint problem that has to be solved numerically. We note that the dual problem is always a linear one, such that in the case of a nonlinear partial differential equation the numerical costs for solving the dual problem requires much less work. If the primal solution is obtained by a Newton iteration then solving the dual problem corresponds to one additional Newton iteration in each time step. From the error representation for the goal quantity localized error indicators can be derived (cf. [3] for details), similarly to the traditional residual-based approach. However, the sharpess of the resulting a posteriori error estimate can not be guaranted anymore as soon as estimates are applied to the error identity.

Even though the DWR approach has been applied to many classes of partial differential equations, our feeling is that its potential for the numerical approximation of convection-dominated problems and stabilized discretizations has not been completely understood and explored yet. In the application of the DWR method the efficient and fast solution of the auxiliary dual problem and the localization of the error estimator is an essential step in practice; cf. e.g., [11, 3, 4, 43, 45]. The dual solution impacts the weights of the resulting error indicators. It is well knwon that the proper choice of the weights is crucial for the effectivity of the adaptation process. They should in particular measure the influence of a present cell on the requested goal quantity of interest. The approximation of the dual solution cannot be done in the finite element space of the primal problem since it would result in a useless vanishing approximation of the error quantity; cf. [3]. Therefore, several techniques of approximation the dual solution efficienty were developed and proposed in the literature. Approximation by a higher-order method, approximation by a higher-order interpolation, approximation

by difference quotients and approximation by local residual problems are known approaches [11, 4, 3, 45]. In particular, higher-order interpolation is applied often in the literature; cf., e.g., [4, 45] .

In this work we combine the DWR approach with stabilized approximations of convection-dominated problems. The adaptive mesh refinement process is directly based on the global error representation, up to higher order error contributions, without estimating the error terms further, i.e. without providing the usual upper bouds for the error in the goal quantity. Thereby we aim to reduce additional approximation errors and non-sharp estimates of standard error indicators and to apply the DWR approach as strictly as possible in order to get a reliable quantification and control of the error in the goal quantity instead of providing only error indicators for an economical mesh adaption strategy. In our approach the dual problem is solved by using higher oder finite element techniques. In numerical experiments we will illustrate the high impact of the proper choice of the weights and thereby of the dual solution on the mesh adaption process. Our overall motivation is to reduce sources of inaccuracies and non-sharp estimates in the a posteriori error control mechanism as far as possible in order to avoid numerical artefacs and a loss of quality in the approximation of the solution and the error control in regions with sharp fronts where highly sensitive solution profiles are present and interpolations are defective. We expect that this strategy allows us to exploit the full potential of the DWR method for the a posteriori quantification of discretization errors. This is in contrast to other works of the literature on the DWR method where much effort is put in the reduction of the computation costs for solving the dual problem. Thereby, the high impact of the dual solution on the error control and mesh generation process is not focused as strongly as in this work. Due to the specific character of convection-dominated problems we are convinced that the error control needs a particular care in regions with interior and boundary layers and in regions with sharp fronts in order to get an accurate quantification of numerical errors. For problems with simpler structures of solutions more economical approximations of the dual solution might be sufficient and appropriate.

This work is organized as follows. In Section 2, we introduce our model problem together with some global assumptions and our notation. Further we present the finite element approximation of this problem and the stabilization of the discretization by using the SUPG method . In Section 3 our a posterior error control mechanism based on the DWR method is developed and localized error terms are derived. In Section 4 some implementational issues are addressed. Finally, in Section 5 the results of numerical computations are presented in order to illustrate the feasibilty, potential and benefit of the proposed approach. Further, a careful comparison with reference values of the literature is given for a benchmark problem.

2. Problem formulation and stabilized discretization

In this work we study the linear convection-diffusion-reaction problem

$$\begin{aligned} \partial_t u + \boldsymbol{b} \cdot \nabla u - \nabla \cdot (\varepsilon \nabla u) + \alpha u &= f \quad \text{in } \Omega \times (0,T]\,, \\ u(\boldsymbol{x},t) &= 0 \quad \text{on } \partial\Omega \times (0,T]\,, \\ u(\boldsymbol{x},0) &= u_0 \quad \text{in } \Omega\,. \end{aligned} \tag{2.1}$$

We assume that $\Omega \subset \mathbb{R}^d$, with $d = 2$ or $d = 3$, is a polyhedral bounded domain and let $I := (0,T]$. For simplicity, problem (2.1) is equipped with homogeneous boundary conditions. Problem (2.1) is considered as a prototype model for more sophistcated equations of practical interest, for instance, for the Navier–Stokes equations of incompressible viscous flow. For an application of our approach to semilinear problems with nonlinear reactive terms we refer to [46].

To ensure the well-posedness of problem (2.1) we assume that $\alpha \in \mathbb{R}_0^+$, $\varepsilon \in \mathcal{L}^\infty(\Omega)$, $\boldsymbol{b} \in \boldsymbol{\mathcal{H}}^1(\Omega) \cap \boldsymbol{\mathcal{L}}^\infty(\Omega)$ with $\varepsilon(x) \geq \varepsilon_0 > 0$ and $(\nabla \cdot \boldsymbol{b})(x) = 0$ almost everywhere in Ω. Further, we let $f \in \mathcal{L}^2\left(0,T;\mathcal{H}_0^{-1}(\Omega)\right)$ and $u_0 \in \mathcal{L}^2(\Omega)$ with $\mathcal{H}_0^{-1}(\Omega)$ denoting the dual space of $\mathcal{H}_0^1(\Omega)$. Then the existence and uniqueness of a weak solution

$$u \in \mathcal{X} := \left\{ v \in \mathcal{L}^2\left(0,T;\mathcal{H}_0^1(\Omega)\right) \mid \partial_t v \in \mathcal{L}^2\left(0,T;\mathcal{H}^{-1}(\Omega)\right) \right\} \tag{2.2}$$

of problem (2.1), satisfying $u(0) = u_0$ and

$$\langle \partial_t u, \varphi \rangle + \langle \boldsymbol{b} \cdot \nabla u, \varphi \rangle + \langle \varepsilon \nabla u, \nabla \varphi \rangle + \langle \alpha u, \varphi \rangle = \langle f, \varphi \rangle \tag{2.3}$$

for all $\varphi \in \mathcal{H}_0^1(\Omega)$ and almost every $t \in (0,T)$, is ensured [20, 40].

The dual weighted residual approach (for short DWR method) is based on a variational space-time discretization of problem (2.5) and of a corresponding adjoint (or dual) problem. In the analysis that is given below we need discontinuous and continuous variational discretizations of the time variable. The discretization and the application of the DWR method is done for variational space-time approximations with piecewise polynomials of arbitrary order in space and time. In our numerical calculations (cf. Section 5) we restrict ourselves to applying lowest order members of these families of time discretization schemes to the primal and dual problem. In this work we aim to demonstrate and analyze the feasibilty of our approach to convection-dominated transport. For higher order variational discretizations of the time variable the solution of the arising algebraic systems of equations becomes much more involved. For their application in non-adaptive computations we refer to, e.g., [7, 35, 6].

For the discretization in time we divide the time interval I into not necessarily equidistant subintervals $I_m := (t_{m-1}, t_m]$, with $m = 1, \ldots, M$, where $0 = t_0 < t_1 < \ldots < t_{M-1} < t_M = T$ with step size $k_m = t_m - t_{m-1}$ and $k = \max_m k_m$. We put

$$\mathcal{Y} := \left\{ \mathcal{L}^2\left(0,T;\mathcal{H}_0^1(\Omega)\right) \mid v_{|I_m} \in C(\overline{I}_m;\mathcal{H}_0^1(\Omega)) \right\}\,. \tag{2.4}$$

Here, the notation $v_{|I_m} \in C(\overline{I}_m; \mathcal{H}_0^1(\Omega))$ means that $v_{|I_m}$ posses a continuous extension to the closure $\overline{I}_m$ of I_m. The unique solution $u \in \mathcal{X}$ of problem (2.3) then satisfies the variational space-time problem: *Find $u \in \mathcal{X}$ such that*

$$\langle\langle \partial_t u, \varphi \rangle\rangle + a(u)(\varphi) + \langle u(0), \varphi(0) \rangle = F(\varphi) + \langle u_0, \varphi(0) \rangle \tag{2.5}$$

for all $\varphi \in \mathcal{Y}$.

In (2.5) we use the notation

$$a(v)(\varphi) := \langle\langle \boldsymbol{b} \cdot \nabla v, \varphi \rangle\rangle + \langle\langle \varepsilon \nabla v, \nabla \varphi \rangle\rangle + \langle\langle \alpha v, \varphi \rangle\rangle \tag{2.6}$$

for $v, \varphi \in \mathcal{Y}$ and

$$F(\varphi) := \langle\langle f, \varphi \rangle\rangle \tag{2.7}$$

for $\varphi \in \mathcal{Y}$, where

$$\langle\langle v, w \rangle\rangle := \int_0^T \langle v, w \rangle \, \mathrm{d}t$$

is the inner product of $\mathcal{L}^2(0,T;\mathcal{L}^2(\Omega))$ and $\langle \cdot, \cdot \rangle$ is the inner product of $\mathcal{L}^2(\Omega)$. In (2.5) the initial condition is imposed in a weak form. We note that $\mathcal{Y}$ is a dense subspace of $\mathcal{L}^2\left(0,T;\mathcal{H}_0^1(\Omega)\right)$.

Next, we introduce the time discrete function spaces

$$\mathcal{X}_k^r := \left\{ v_k \in \mathcal{L}^2\left(0,T;\mathcal{H}_0^1(\Omega)\right) \mid v_{k|I_m} \in \mathcal{P}_r\left(I_m;\mathcal{H}_0^1(\Omega)\right),\ v_k(0) \in \mathcal{L}^2(\Omega) \right\}, \tag{2.8}$$

$$\overline{\mathcal{X}}_k^r := \left\{ v_k \in C\left([0,T];\mathcal{L}^2(\Omega)\right) \mid v_{k|I_m} \in \mathcal{P}_r\left(I_m;\mathcal{H}_0^1(\Omega)\right) \right\}, \tag{2.9}$$

where $\mathcal{P}_r(I_m;\mathcal{H}_0^1(\Omega))$ denotes the space of all polynomials in time up to degree $r \geq 0$ on I_m with values in $\mathcal{H}_0^1(\Omega)$. For some function $v_k \in \mathcal{X}_k^r$ we define the limits $v_{k,m}^{\pm}$ from above and below of v_k at t_m as well as their jump at t_m by

$$v_{k,m}^{\pm} := \lim_{s \to 0} v_k(t_m \pm s), \qquad [v_k]_m := v_{k,m}^+ - v_{k,m}^-.$$

For the temporal discretization of the primal problem (2.5) we use the discontinuous Galerkin method (for short dG(r)); cf. [47]. The time-discrete variational approximation of problem (2.5) then reads as follows: *Find $u_k \in \mathcal{X}_k^r$ such that*

$$A(u_k)(\varphi_k) + \left\langle u_{k,0}^-, \varphi_{k,0}^- \right\rangle = F(\varphi_k) + \left\langle u_0, \varphi_{k,0}^- \right\rangle \tag{2.10}$$

for all $\varphi_k \in \mathcal{X}_k^r$.

In (2.10) we use the notation

$$A(v_k)(\varphi_k) := \sum_{m=1}^{M} \int_{I_m} \langle \partial_t v_k, \varphi_k \rangle \, \mathrm{d}t + a(v_k)(\varphi_k) + \sum_{m=0}^{M-1} \left\langle [v_k]_m, \varphi_{k,m}^+ \right\rangle \tag{2.11}$$

for $v_k, \varphi_k \in \mathcal{X}_k^r$. We note that the initial condition is incorporated into the variational problem. For the derivation and an analysis of the dG(r) semidiscretization of

abstract evolution problems in Hilbert spaces we refer to [47]. The dG(r) method is nonconforming, since by an embedding result (cf. [16]) it holds that $\mathcal{X}_k^r \not\subset \mathcal{X}$.

Next, we describe the Galerkin finite element approximation in space of the semidiscrete problem (2.10). To this end, we use two- or three-dimensional shape- and contact-regular meshes [15]. By $\mathcal{T}_h = \{K\}$ we denote a conforming decomposition of the domain Ω into triangles in two space dimensions or tetrahedra in three space dimensions. Quadrilateral and hexahedral elements can be applied in the same way by means of the standard modifications. On $\mathcal{T}_h$ we define the function space $\mathcal{V}_h^p \subset \mathcal{H}_0^1(\Omega)$ by

$$\mathcal{V}_h^p := \{v \in \mathcal{H}_0^1(\Omega) \cap \mathcal{C}(\bar{\Omega}) \mid v_{|K} \in \mathcal{P}_p(K)\ \forall K \in \mathcal{T}_h\}\,,$$

with $\mathcal{P}_p(K)$ denoting the function space of polynomials of degree at most p on K. By replacing $\mathcal{H}_0^1(\Omega)$ in the definition of the semidiscrete function spaces $\mathcal{X}_k^r$ and $\overline{\mathcal{X}}_k^r$ in (2.8) and (2.9), respectively, by $\mathcal{V}_h^p$, we obtain the fully discrete function space

$$\mathcal{X}_{kh}^{r,p} := \left\{v_{kh} \in \mathcal{X}_k^r \mid v_{|I_m} \in \mathcal{P}_r(I_m; \mathcal{V}_h^{p,m}),\ \text{for } m = 1, \ldots, M\,,\ v_{kh}(0) \in V_h^p\right\} \tag{2.12}$$

with $\mathcal{X}_{kh}^{r,p} \subset \mathcal{X}_k^r$. We note that the spatial finite element space $\mathcal{V}_h^{p,m}$ is allowed to be different on all intervals I_m which is natural in the context of a discontinuous Galerkin approximation of the time variable and allows dynamic mesh changes in time. Throughout the time steps k_m are kept constant in space. The fully discrete discontinuous in time scheme that is studied below then reads as follows: *Find* $u_{kh} \in \mathcal{X}_{kh}^{r,p}$*, such that*

$$A(u_{kh})(\varphi_{kh}) + \left\langle u_{kh,0}^-, \varphi_{kh,0}^- \right\rangle = F(\varphi_{kh}) + \left\langle u_0, \varphi_{kh,0}^- \right\rangle \tag{2.13}$$

for all $\varphi_{kh} \in \mathcal{X}_{kh}^{r,p}$ *with* $A(\cdot)(\cdot)$ *and* $F(\cdot)$ *being defined in* (2.11) *and* (2.7)*, respectively.*

In the DWR approach a continuous Galerkin approximation of the time variable is also needed. This type of discretization is applied below to the adjoint problem of (2.5). Here we introduce the continuous Galerkin approximation of the time variable and the resulting fully discrete finite element method for the primal problem (2.5) in order to illustrate its definition. The formulation of the continuous Galerkin approximation on dynamically changing meshes is more involved since the global continuity of functions in the trial space has to be ensured. Let $\{\tau_0, \ldots, \tau_r\}$ be a basis of $\mathbb{P}_r(I_m; \mathbb{R})$ that satisfies the conditions

$$\tau_0(t_{m-1}) = 1\,, \quad \tau_0(t_m) = 0\,, \quad \tau_i(t_{m-1}) = 0\,,\ \ i = 1, \ldots, r\,.$$

Then we define

$$\mathcal{X}_{kh}^{r,p,m} = \operatorname{span}\left\{\tau_i v_i \mid v_0 \in \mathcal{V}_h^{p,m-1}\,,\ v_i \in \mathcal{V}_h^{p,m}\,,\ i = 1, \ldots, r\right\}$$

and

$$\overline{\mathcal{X}}_{kh}^{r,p} := \left\{v_{kh} \in C(\overline{I}; \mathcal{L}^2(\Omega)) \mid v_{kh|I_m} \in \mathcal{X}_{kh}^{r,p,m}\right\} \subset \overline{\mathcal{X}}_k^r\,.$$

We note that this definition of the trial space $\overline{\mathcal{X}}_{kh}^{r,p}$ ensures the continuity of its functions. This is due to the fact that the vanishing spatial degrees of freedom in $\mathcal{V}_h^{p,m-1}$

are coupled only with the temporal basis function τ_0 that vanishes in the right end endpoint t_m of I_m. The fully discrete continuous in time scheme that is applied below then reads as follows: *Find* $u_{kh} \in \overline{\mathcal{X}}_{kh}^{r,p}$, *such that*

$$\langle\langle \partial_t u_{kh}, \varphi_{k,h} \rangle\rangle + a(u_{kh})(\varphi_{kh}) + \langle u_{kh}(0), \varphi_{kh,0}^- \rangle = \langle\langle f, \varphi_{kh} \rangle\rangle + \langle u_0, \varphi_{kh,0}^- \rangle \tag{2.14}$$

for all $\varphi_{kh} \in \mathcal{X}_{kh}^{r-1,p}$.

In (2.14) the initial condition is imposed in weak form. This scheme belongs to the class of Petrov–Galerkin methods since the spaces for the trial and test functions differ.

In this work we focus on convection-dominated problems with small diffusion parameter $0 < \varepsilon_0 \ll 1$. Then the finite element approximation needs to be stabilized in order to reduce spurious and non-physical oscillations of the discrete solution arising close to layers. Here, we apply the streamline upwind Petrov–Galerkin method (for short SUPG); cf. [44, 33, 8]. The stabilized variant of the fully discrete scheme (2.13) then reads as follows: *Find* $u_{kh} \in \mathcal{X}_{kh}^{r,p}$ *such that*

$$A_S(u_{kh})(\varphi_{kh}) + \left\langle u_{kh,0}^-, \varphi_{k,0}^- \right\rangle = F(\varphi_{kh}) + \left\langle u_0, \varphi_{kh,0}^- \right\rangle \tag{2.15}$$

for all $\varphi_{kh} \in \mathcal{X}_{kh}^{r,p}$.

In (2.15) we put

$$A_S(u_{kh})(\varphi_{kh}) := A(u_{kh})(\varphi_{kh}) + S(u_{kh})(\varphi_{kh})$$

with

$$\begin{aligned} S(u_{kh})(\varphi_{kh}) := & \sum_{m=1}^{M} \int_{I_m} \sum_{K \in \mathcal{T}_h} \delta_K \langle R(v_{kh}), \boldsymbol{b} \cdot \nabla \varphi_{kh} \rangle_K \, \mathrm{d}t \\ & + \sum_{m=0}^{M-1} \sum_{K \in \mathcal{T}_h} \delta_K \left\langle [u_{kh}]_m, \boldsymbol{b} \cdot \nabla \varphi_{kh,m}^+ \right\rangle_{\mathcal{L}^2(K)} \\ & + \sum_{K \in \mathcal{T}_h} \delta_K \left\langle u_{kh,0}^- - u_0, \boldsymbol{b} \cdot \nabla \varphi_{kh,0}^- \right\rangle_{\mathcal{L}^2(K)}, \end{aligned} \tag{2.16}$$

$$R(u_{kh}) := \partial_t u_{kh} + \boldsymbol{b} \cdot \nabla u_{kh} - \nabla \cdot (\varepsilon \nabla u_{kh}) + \alpha u_{kh} - f \,.$$

for $\{u_{kh}, \varphi_{kh}\} \in \mathcal{X}_{kh}^{r,p} \times \mathcal{X}_{kh}^{r,p}$. In Eq. (2.16) we denote by $\langle \cdot, \cdot \rangle_{\mathcal{L}^2(K)}$ the inner product of the space $\mathcal{L}^2(K)$. The proper choice of the stabilization parameter δ_K is an important issue in the application of the SUPG approach; cf. [31] and the discussion therein. As proposed by our analysis of stabilized finite element methods in [8] we choose

$$\delta_K \sim \min \left\{ \frac{h_K}{p \|\boldsymbol{b}\|_{\boldsymbol{\mathcal{L}}^\infty(K)}}; \frac{h_K^2}{p^4 \, \varepsilon}; \frac{1}{k_m + \alpha}; \frac{k_m + \alpha}{\alpha^2} \right\}$$

In (2.16) and from now on we assume for brevity that the diffusion coefficient $\varepsilon(x)$ equals a constant ε. Otherwise the additional projection operator that is used in [8]

has to be applied to the diffusive term of the residual in (2.16). The SUPG stabilized form of the continuous in time scheme (2.14) is obtained along the same lines.

Remark 2.1. *In this work we restrict ourselves to linear problems in the nonstationary case. This is sufficient to study and illustrate our dual weighted residual approach for stabilized finite element approximations of convection-dominated problems. A further stabilization in crosswind direction may be obtained by using an additional shock-capturing stabilization technique; cf., e.g. [8, 33, 30]. However, the most efficient family of this type of additional stabilization is based on adding additional nonlinear terms. In the case of linear problems the latter methods then increase the complexity of solving the arising algebraic system of equations significantly. For this reason an additional shock-capturing stabilization is not studied here for the nonstationary problem* (2.1)*. However, some of our numerical studies that are presented in Section 5 are done for steady nonlinear problems. Restricting ourselves to steady problems in the nonlinear case is sufficient to demonstrate the feasibilty of our method also to nonlinear equations and helps to separate characteristic features that are related to the discretization in space.*

For the steady counterpart of problem (2.1),

$$\alpha u + \boldsymbol{b}\cdot\nabla u - \nabla\cdot(\varepsilon\nabla u) + r(u) = f \quad \text{in } \Omega, \qquad u = 0 \quad \text{on } \partial\Omega\,, \tag{2.17}$$

with the above assumptions about the data and, further, supposing that (cf. [8])

$$r \in C^1(\mathbb{R})\,, \quad r(0) = 0\,, \quad r'(s) \geq r_0 \geq 0 \quad \text{for } s \geq 0\,,\ s \in \mathbb{R}\,,$$

we consider using SUPG and additional shock-capturing stabilization (cf. [8, 30]) such that the fully discrete problem reads as: *Find* $u_h \in \mathcal{V}_h^p$ *such that*

$$A_{SC}(u_h)(\varphi_h) = F(\varphi_h) \tag{2.18}$$

for all $\varphi_h \in \mathcal{V}_h^p$ *with*

$$\begin{aligned}
A_{SC}(u_h)(\varphi_h) &:= A(u_h)(\varphi_h) + S(u_h)(\varphi_h) + S_C(u_h)(\varphi_h)\,,\\
A(u_h)(\varphi_h) &= \langle \alpha u_h, \varphi_h\rangle + \langle \boldsymbol{b}\cdot\nabla u_h, \varphi_h\rangle + \langle \varepsilon\nabla u_h, \nabla\varphi_h\rangle + \langle r(u_h), \varphi_h\rangle\\
S(u_h)(\varphi_h) &:= \sum_{K\in\mathcal{T}_h} \delta_K \langle R(u_h), \boldsymbol{b}\cdot\nabla\varphi_h\rangle_{\mathcal{L}^2(K)}\,,\\
R(u_h) &:= \alpha u_h + \boldsymbol{b}\cdot\nabla u_h - \nabla\cdot(\Pi_K\varepsilon\nabla u_h) + r(u_h) - f\,,\\
S_C(u_h)(\varphi_h) &:= \sum_{K\in\mathcal{T}_h} \langle \tau_K(u_h)\boldsymbol{D}\nabla u_h, \nabla\varphi_h\rangle_{\mathcal{L}^2(K)}\,.\\
F(\varphi_h) &:= \langle f, \varphi_h\rangle
\end{aligned} \tag{2.19}$$

and the stabilization parameter

$$\delta_K \sim \min\left\{\frac{h_K}{p\|\boldsymbol{b}\|_{\boldsymbol{\mathcal{L}}^\infty(K)}}; \frac{h_K^2}{p^4\mu_{\text{inv}}^2\|\varepsilon\|_{\mathcal{L}^\infty(K)}}; \frac{1}{\alpha+r_0}; \frac{\alpha+r_0}{L_r^2}\right\}\ ,,$$

$$\tau_K(u_h) := l_K(u_h)\hat{R}_K(u_h) = \frac{l_K(u_h)\|R(u_h)\|_{\mathcal{L}^2(K)}}{|u_h|_{\mathcal{H}^1(K)}+\kappa_K}\,, \tag{2.20}$$

$$l_K(u_h) := l_0 h_K \max\left\{0, \beta - \frac{2\|\varepsilon\|_{\mathcal{L}^\infty(K)}}{h_K\hat{R}_K(u_h)}\right\}\,, \quad \boldsymbol{D} := \begin{cases} \boldsymbol{I} - \dfrac{\boldsymbol{b}\otimes\boldsymbol{b}}{|\boldsymbol{b}|^2}\,, & \boldsymbol{b}\neq\boldsymbol{0}\,, \\ \boldsymbol{0}\,, & \boldsymbol{b}=\boldsymbol{0}\,. \end{cases}$$

In set the of equations (2.20) we denote by $\|\cdot\|_{\mathcal{L}^\infty(K)}$ and $\|\cdot\|_{\mathcal{H}^1(K)}$ the usual norms associated with the function spaces on the element K. For further details regarding the definition and choice of the stabilization parameter in (2.20) we refer to [8].

3. A dual weighted residual approach for stabilized finite element methods

Here we develop our application of the dual weighted residual (for short DWR) method (cf. [3]) to the stabilized finite element approximation (2.14) of problem (2.1). The DWR approach aims at an error control for an arbitrary quantity of physical interest. This is contrast to standard a posteriori error estimates that typically provide computable upper (and lower) bounds in terms of numerically available quantities for the numerical approximation errors measured in standard norm, for instance in the natural norm of the discretization for that an a priori error analysis is available. The capability of providing an error control mechanism for physically relevant quantities offers large potential of the DWR approach in engineering scienes. The DWR method is based on duality techniques and an additional nonstationary adjoint problem has to be solved which includes the primal solution as coefficient. Thus, in each adaptation step of an adaptive algorithm numerical approximations to the solution of the primal and dual problem need to be computed for the whole time period such that the simulations become numerically expensive. Several techniques were proposed to reduce the computational costs for determing the approximate dual solution. For this topic we refer to the discusssion in Section 1.

The characteristic feature of most of the existing a posteriori error analyses for convection-dominated is their non-robustness with respect to the small perturbation parameter which then leads to adaptive meshes that are not satisfactory yet. On the other hand the DWR method yields an exact representation of the discretization error in the target quantity. This observation is the key point of our application of the DWR concept. The latter representation depends on the exact dual solution that has still to be approximated. For this we use higher order techniques which is in contrast to other works of the literatur [3]. Thereby we aim at a reduction of approximation errors in

the sensitive regions of convection-dominated problems with sharp layers and strong gradients where approximations and interpolations are highly delicious and strongly defective. This approach increases the computational costs for solving the adjoint problem, but on the other hand it improves the approximation quality of the weights in the a posteriori error control mechanism and, thereby, the effectivity of the adaptation process. The proper choice of the weights is considered to be an important step in the application of the DWR method to stabilized approximations of convection-dominated problems and to deserve careful attention. Our numerical computations (cf. Section 5) will illustrate the impact of the approximation of the dual solution on the approximation quality in the target quantity.

The DWR approach aims to control the error with respect so some output functional $J(\cdot)$. This requires a respresentation of an estimate of the difference $J(u) - J(u_{kh})$. Here, $J(u)$ is the user-chosen target quantity of physical interest. We suppose that the functional $J(\cdot)$ is defined on the space $\mathcal{Y}$ introduced in (2.4), i.e. $\mathcal{J} : \mathcal{Y} \mapsto \mathbb{R}$. Further, we assume that the functional $\mathcal{J}$ is Fréchet differentiable, i.e. $J'(y) \in \mathcal{Y}'$ for $y \in \mathcal{Y}$. Moreover, we assume that the directional derivative of J admits an $\mathcal{L}^2$ representation such that for any $v \in \mathcal{Y}$ there exists some function $j(v) \in \mathcal{L}^2\left(0, T; \mathcal{L}^2(\Omega)\right)$ such that

$$\mathcal{J}'(v)(\varphi) = \langle\langle j(v), \varphi \rangle\rangle \tag{3.1}$$

is satisfied for all $\varphi \in \mathcal{Y}$. If the target functional J is less regular, involving for example spatial or temporal point values, then the theory developed below can no longer be applied directly. In this case a regularization of the functional may be used to overcome the lack of regularity. However, the regularization is usually only necessary in the development of the formal framework. On the discrete level and in practical computations the abstract theory often performs successfully even for less regular output functionals (cf. Section 5).

For the derivation of an a posteriori error representation for $J(u) - J(u_{kh})$ we employ the Euler–Lagrange method of constrained optimization. We define the Lagrangian functional $\mathcal{L} : \mathcal{X} \times \mathcal{Y} \mapsto \mathbb{R}$ by

$$\mathcal{L}(u, z) := \mathcal{J}(u) + F(z) - \langle\langle \partial_t u, z \rangle\rangle - a(u)(z) - \langle u(0) - u_0, z(0) \rangle \tag{3.2}$$

with the target quantity $\mathcal{J}(\cdot)$ and the forms $a(\cdot)(\cdot)$ and $F(\cdot)$ being defined in (2.6) and (2.7), respectively. A stationary point $\{u, z\}$ of $\mathcal{L}(\cdot, \cdot)$ on $\mathcal{X} \times \mathcal{Y}$ is determined by

$$\mathcal{L}'(u, z)(\psi, \varphi) = 0 \qquad \text{for all } \{\psi, \varphi\} \in \mathcal{X} \times \mathcal{Y}\,, \tag{3.3}$$

or equivalently by the system of equations

$$\langle\langle \partial_t \psi, z \rangle\rangle + a(\psi)(z) + \langle \psi(0), z(0) \rangle = J'(u)(\psi) \qquad \text{for all } \psi \in \mathcal{X}\,, \tag{3.4}$$

$$\langle\langle \partial_t u, \varphi \rangle\rangle + a(u)(\varphi) + \langle u(0), \varphi(0) \rangle = F(\varphi) + \langle u_0, \varphi(0) \rangle \qquad \text{for all } \varphi \in \mathcal{Y}\,. \tag{3.5}$$

The second of these equations, the z-component of the stationarity condition, is just the given primal problem (2.5). Equation (3.4), the u-component of the stationarity

condition, is called the dual or adjoint equation. In particular, the solution $z \in \mathcal{Y}$ of the adjoint problem (3.4) can be recovered as the solution of the following variational problem: *Find* $z \in \mathcal{X}$ *with*

$$\begin{aligned} -\langle\langle \partial_t z, \psi \rangle\rangle - \langle\langle \boldsymbol{b} \cdot \nabla z, \psi \rangle\rangle + \langle\langle \varepsilon \nabla z, \nabla \psi \rangle\rangle \\ + \langle\langle \alpha z, \psi \rangle\rangle + \langle z(T), \psi(T) \rangle = J'(u)(\psi) \end{aligned} \tag{3.6}$$

for all $\psi \in \mathcal{Y}$.

Under the hypothesis (3.1) the dual problem (3.6) has the structure of the primal problem (2.5) but running backward in time. The existence and uniqueness of a solution $z \in \mathcal{X}$ of problem (3.6) is thus ensured by the same setting and arguments as used for the primal problem (2.5). For a right-hand side term (3.1) and appropriate assumptions about the boundary $\partial\Omega$ of Ω the continuity constraint in the definition (2.4) of $\mathcal{Y}$ holds (cf. [20] and [40] for the Sobolev embedding results) such that $z \in \mathcal{Y}$ is ensured. To see that the solution of (3.6) in fact satisfies the variational problem (3.4), we use integration by part with respect to the time variable to find that

$$-\langle\langle \partial_t z, \psi \rangle\rangle = \langle z(0), \psi(0) \rangle - \langle z(T), \psi(T) \rangle + \langle\langle \partial_t \psi, z \rangle\rangle \tag{3.7}$$

for test functions $\psi \in \mathcal{X}$. Combining (3.6) with (3.7) and using integration by parts in the convective term yields (3.4). Below, our application of the DWR approach is built upon the dual problem (3.6).

Remark 3.1. *In the context of our stabilized finite element approximations two different approaches of applying the DWR method can be used. The first approach, refered to as the* ***first stabilize and then dualize*** *method, is obtained by introducing a discrete Lagrangian functional* $\widetilde{\mathcal{L}}$*, that is associated with the stabilized Galerkin discretization* (2.15)*, and defining the discrete solution* $\{u_{kh}, z_{kh}\} \in \mathcal{X}_{kh}^{r,p} \times \mathcal{X}_{kh}^{r,p}$ *as the stationary point of* $\widetilde{\mathcal{L}}$ *on* $\mathcal{X}_{kh}^{r,p} \times \mathcal{X}_{kh}^{r,p}$*. To find the desired representation of the error* $J(u) - J(u_{kh})$*, this quantity is represented in terms of the error in the discrete Lagrangian functional; cf. [45]. The second approach, refered to as the* ***first dualize and then stabilize*** *method, is obtained by discretizing the continuous Euler–Lagrange system* (3.4), (3.5) *by means of the proposed stabilized Galerkin discretization scheme* (2.15)*, i.e., that the discontinuous in time and continuous in space finite element method along with the SUPG stabilization in space is applied to the system of equations* (3.4), (3.5)*. As it is shown below, the discrete solution* $\{u_{kh}, z_{kh}\} \in \mathcal{X}_{kh}^{r,p} \times \mathcal{X}_{kh}^{r,p}$ *is then no longer a stationary point of the Lagrangian functional, it's just an approximation to such point. In this approach the error in the goal quantity* $J(u) - J(u_{kh})$ *is represented in terms of the continuous Lagrangian functional* (3.2)*. The difference of the either approaches comes through the presence of the stabilization terms in the discrete Lagrangian functional. In this work we apply the second approach. In the second approach the SUPG stabilization of the discrete dual problem is based on the residual of the discrete counterpart of the backward in time problem* (3.6)*; cf. Eq.* (3.9) *below. This seems to be more natural. Moreover, numerical instabilities were observed in the literature [9] for the first strategy of transposing the whole stabilized system. For a careful comparison of*

the either approaches of applying the DWR method to stabilized discretization schemes we refer to [46] where this is done for stationary problems. For illustration purposes we sketch both approaches briefly. Then we follow the second one. We note that the resulting numerical scheme differ in general since dualization (i.e. optimization) and stabilization do not commute.

First Stabilize and Then Dualize

The discrete Lagrangian functional $\widetilde{\mathcal{L}} : \mathcal{X}_{kh}^{r,p} \times \mathcal{X}_{kh}^{r,p} \mapsto \mathbb{R}$ associated with the stabilized Galerkin discretization (2.15) is defined by

$$\widetilde{\mathcal{L}}(u_{kh}, z_{kh}) = \mathcal{J}(u_{kh}) + F(z_{kh}) - A_S(u_{kh})(z_{kh}) - \left\langle u_{kh,0}^- - u_0, z_{kh,0}^- \right\rangle . \tag{3.8}$$

A stationary point $\{u_{kh}, z_{kh}\}$ of $\widetilde{\mathcal{L}}(\cdot,\cdot)$ on $\mathcal{X}_{kh}^{r,p} \times \mathcal{X}_{kh}^{r,p}$ is determined by the equation

$$\widetilde{\mathcal{L}}'(u_{kh}, z_{kh})(\psi_{kh}, \varphi_{kh}) = 0 \qquad \text{for all } \{\psi_{kh}, \varphi_{kh}\} \in \mathcal{X}_{kh}^{r,p} \times \mathcal{X}_{kh}^{r,p} ,$$

or equivalently by the system of equations

$$A_S(\psi_{kh})(z_{kh}) + \left\langle \psi_{kh,0}^-, z_{kh,0}^- \right\rangle = J'(u_{kh})(\psi_{kh}) \qquad \text{for all } \psi_{kh} \in \mathcal{X}_{kh}^{r,p} ,$$

$$A_S(u_{kh})(\varphi_{kh}) + \left\langle u_{kh,0}^-, \varphi_{kh,0}^- \right\rangle = F(\varphi_{kh}) + \left\langle u_0, \varphi_{kh,0}^- \right\rangle \qquad \text{for all } \varphi_{kh} \in \mathcal{X}_{kh}^{r,p} .$$

First Dualize and Then Stabilize

We discretize the continuous Euler–Lagrange system (3.4), (3.5) by the proposed stabilized Galerkin discretization scheme (2.15). Then the identity (3.5) yields the discrete primal problem (2.15): *Find* $u_{kh} \in \mathcal{X}_{kh}^{r,p}$ *such that*

$$A_S(u_{kh})(\varphi_{kh}) + \left\langle u_{kh,0}^-, \varphi_{k,0}^- \right\rangle = F(\varphi_{kh}) + \left\langle u_0, \varphi_{kh,0}^- \right\rangle \quad \text{for all } \varphi_{kh} \in \mathcal{X}_{kh}^{r,p} . \tag{3.9}$$

From the continuous dual problem (3.4), rewritten in the form (3.6), we find by using the proposed stabilized Galerkin discretization scheme (2.15) the following discrete dual problem: *Find* $z_{kh} \in \mathcal{X}_{kh}^{r,p}$ *such that*

$$A_S^*(z_{kh})(\psi_{kh}) + \left\langle z_{kh,T}^-, \psi_{kh,T}^- \right\rangle = \mathcal{J}'(u_{kh})(\psi_{kh}) \quad \text{for all } \psi_{kh} \in \mathcal{X}_{kh}^{r,p} . \tag{3.10}$$

Further, we define $z_{kh}(0) = z_{k,0}^+$. In (3.10) we put

$$A_S^*(z_{kh})(\psi_{kh}) := A^*(z_{kh})(\psi_{kh}) + S^*(z_{kh})(\psi_{kh})$$

with

$$\begin{aligned} A^*(z_{kh})(\psi_{kh}) := \sum_{m=1}^{M} - \int_{I_m} \langle \partial_t z_{kh}, \psi_{kh} \rangle \, \mathrm{d}t - \langle\langle b \cdot \nabla z_{kh}, \psi_{kh} \rangle\rangle + \langle\langle \varepsilon \nabla z_{kh}, \nabla \psi_{kh} \rangle\rangle \\ + \langle\langle \alpha z_{kh}, \psi_{kh} \rangle\rangle - \sum_{m=0}^{M-1} \left\langle [z_{kh}]_m , \psi_{kh,m}^+ \right\rangle \end{aligned} \tag{3.11}$$

and

$$S^*(z_{kh})(\psi_{kh}) := \sum_{m=1}^{M} \int_{I_m} \sum_{K\in\mathcal{T}_h} \delta_K^* \langle R^*(z_{kh}), \boldsymbol{b}\cdot\nabla\psi_{kh}\rangle_K \,\mathrm{d}t$$
$$- \sum_{m=0}^{M-1} \sum_{K\in\mathcal{T}_h} \delta_K^* \left\langle [z_{kh}]_m, \boldsymbol{b}\cdot\nabla\psi^+_{kh,m}\right\rangle_{\mathcal{L}(K)} + \sum_{K\in\mathcal{T}_h} \delta_K^* \left\langle z^-_{kh,M}, \boldsymbol{b}\cdot\nabla\psi^-_{kh,M}\right\rangle_{\mathcal{L}(K)},$$

$$R^*(z_{kh}) := -\partial_t z_{kh} - \boldsymbol{b}\cdot\nabla z_{kh} - \nabla\cdot(\varepsilon\nabla z_{kh}) + \alpha z_{kh} - j(u_{kh}).$$

In the definiton of the local residual $R(z_{kh})$ we use the assumption (cf. (3.1)) that $J'(u_{kh})(\cdot)$ admits an $\mathcal{L}^2$ respresentation such that $J'(u_{kh})(\psi_{kh}) = \langle\langle j(u_{kh}), \psi_{kh}\rangle\rangle$ is satisfied for all $\psi_{kh} \in \mathcal{X}_{kh}^{r,p}$ with some function $j(u_{kh}) \in \mathcal{L}^2(0,T;\mathcal{L}^2(\Omega))$.

To derive a representation of the error $J(u) - J(u_{kh})$ we need some abstract results. For this we need to extend the definition of the Lagrangian functional to arguments of $(\mathcal{X} + \mathcal{X}_{kh}^{r,p}) \times \mathcal{Y}$. In the following we let $\mathcal{L} : (\mathcal{X} + \mathcal{X}_{kh}^{r,p}) \times \mathcal{Y}$ be defined by

$$\begin{aligned}\mathcal{L}(u,z) :=& \mathcal{J}(u) + F(z) - \sum_{m=1}^{M} \int_{I_m} \langle \partial_t u, z\rangle \,\mathrm{d}t - a(u)(z) \\ &- \sum_{m=0}^{M-1} \left\langle [u]_m, z_m^+\right\rangle - \left\langle u(0)^- - u_0, z(0)^-\right\rangle .\end{aligned} \tag{3.12}$$

Then it follows that

$$\begin{aligned}&\mathcal{L}_u(u,z)(\psi) + \mathcal{L}_z(u,z)(\varphi) \\ &= \mathcal{J}'(u)(\psi) - \sum_{m=1}^{M} \int_{I_m} \langle \partial_t\psi, z\rangle \,\mathrm{d}t - a(\psi)(z) - \sum_{m=0}^{M-1} \left\langle [\psi]_m, z_m^+\right\rangle - \left\langle \psi(0)^-, z(0)^-\right\rangle \\ &\quad + F(\varphi) - \sum_{m=1}^{M} \int_{I_m} \langle \partial_t u, \varphi\rangle \,\mathrm{d}t - a(u)(\varphi) - \sum_{m=0}^{M-1} \left\langle [u]_m, \varphi_m^+\right\rangle - \left\langle u(0)^- - u_0, \varphi(0)^-\right\rangle \\ &= \mathcal{J}'(u)(\psi) + \sum_{m=1}^{M} \int_{I_m} \langle \partial_t z, \psi\rangle \,\mathrm{d}t + \langle\langle \boldsymbol{b}\cdot\nabla z, \psi\rangle\rangle - \langle\langle \varepsilon\nabla z, \nabla\psi\rangle\rangle - \langle\langle \alpha z, \psi\rangle\rangle \\ &\quad + \sum_{m=0}^{M-1} \left\langle [z]_m, \psi_m^-\right\rangle - \left\langle z(T)^-, \psi(T)^-\right\rangle + F(\varphi) - \sum_{m=1}^{M} \int_{I_m} \langle \partial_t u, \varphi\rangle \,\mathrm{d}t \\ &\quad - a(u)(\varphi) - \sum_{m=0}^{M-1} \left\langle [u]_m, \varphi_m^+\right\rangle - \left\langle u(0)^- - u_0, \varphi(0)^-\right\rangle\end{aligned} \tag{3.13}$$

for all $\{\psi,\varphi\} \in (\mathcal{X} + \mathcal{X}_{kh}^{r,p}) \times \mathcal{Y}$.

For the stationary point $\{u, z\}$ of $\mathcal{L}(\cdot,\cdot)$ on $\mathcal{X} \times \mathcal{X}$ that is determined by (3.3) or (3.4), (3.5), respectively, we have that $u, z \in C([0,T]; \mathcal{L}^2(\Omega))$. Therefore it follows that

$$\mathcal{L}_u(u,z)(\psi) + \mathcal{L}_z(u,z)(\varphi) = 0 \tag{3.14}$$

for all $\{\psi, \varphi\} \in \mathcal{X} \times \mathcal{Y}$. The discrete solutions $\{u_{kh}, z_{kh}\} \in \mathcal{X}_{kh}^{r,p} \times \mathcal{X}_{kh}^{r,p}$ then satisfy

$$\begin{aligned} &\mathcal{L}_u(u_{kh},z_{kh})(\psi_{kh}) + \mathcal{L}_z(u_{kh}, z_{kh})(\varphi_{kh}) \\ &\qquad = S(u_{kh})(\varphi_{kh}) + S^*(z_{kh})(\psi_{kh}) - \sum_{m=0}^{M-1} \langle [z_{kh}]_m \,, [\psi_{kh}]_m \rangle \end{aligned} \tag{3.15}$$

for all $\{\psi_{kh}, \varphi_{kh}\} \in \mathcal{X}_{kh}^{r,p} \times \mathcal{X}_{kh}^{r,p}$. For the defect of the discrete solutions in the stationarity condition (3.15) we use the notation

$$\mathcal{D}(x_{kh})(y_{kh}) := S(u_{kh})(\varphi_{kh}) + S^*(z_{kh})(\psi_{kh}) - \sum_{m=0}^{M-1} \langle [z_{kh}]_m \,, [\psi_{kh}]_m \rangle \tag{3.16}$$

with $x_{kh} := \{u_{kh}, z_{kh}\} \in \mathcal{X}_{kh}^{r,p} \times \mathcal{X}_{kh}^{r,p}$ and $y_{kh} := \{\psi_{kh}, \varphi_{kh}\} \in \mathcal{X}_{kh}^{r,p} \times \mathcal{X}_{kh}^{r,p}$.

To derive a representation of the error $J(u) - J(u_{kh})$ we need the following abstract theorem that develops the error in terms of the Lagrangian functional; cf. [46].

Theorem 3.2. *Let X be a function space and $\mathcal{L} : X \mapsto R$ be a three times differentiable functional on X. Suppose that $x_c \in X_c$ with some ("continuous") function space $X_c \subset X$ is a stationary point of $\mathcal{L}$. Suppse that $x_d \in X_d$ with some ("discrete") function space $X_d \subset X$, with not necessarily $X_d \subset X_c$, is a Galerkin approximation to x_c being defined by the equation*

$$\mathcal{L}'(x_d)(y_d) = \mathcal{D}(x_d)(y_d) \tag{3.17}$$

for all $y_d \in X_d$. In addition, suppose that the auxiliary condition

$$\mathcal{L}'(x_c)(x_d) = 0 \tag{3.18}$$

is satisfied. Then there holds the error representation

$$\mathcal{L}(x_c) - \mathcal{L}(x_d) = \frac{1}{2}\mathcal{L}'(x_d)(x_c - y_d) + \frac{1}{2}\mathcal{D}(x_d)(y_d - x_d) + \mathcal{R}\,, \tag{3.19}$$

for all $y_d \in X_d$, where the remainder $\mathcal{R}$ is defined by

$$\mathcal{R} = \frac{1}{2}\int_0^1 \mathcal{L}'''(x_d + se)(e,e,e) \cdot s \cdot (s-1)\,\mathrm{d}s \tag{3.20}$$

with the notation $e := x_c - x_d$.

Proof. In order to keep this work self-contained the proof of Theorem 3.2 is given in the appendix. □

We note that Theorem 3.2 differs from similar theorems that are presented in [3, 4, 45], for instance, since in our case the discrete solution $\{u_{kh}, z_{kh}\} \in \mathcal{X}_{kh}^{r,p} \times \mathcal{X}_{kh}^{r,p}$ is not a stationary point of a Lagrangian functional but only an approximation to such point. In our case the assumption (3.18) is fulfilled by means of (3.13) along with the definition of the function spaces yielding that $\mathcal{X}_{kh}^{r,p} \subset \mathcal{Y}$. Theorem 3.2 now enables us to derive an error representation in terms of the target quantity $J(\cdot)$. Here we do not separate the error of the temporal and spatial discretization. We study directly the error between the continuous and the fully discrete solution which is in contrast to the approach in [45] for instance.

For the representation of the error in terms of the target quantity $J(\cdot)$ we still define the primal residual $\rho(u_{kh})(\cdot)$ and the adjoint residual $\rho^*(z_k)(\cdot)$ by means of

$$\rho(u_{kh})(\varphi) := F(\varphi) - A(u_{kh})(\varphi) - \left\langle u_{kh,0}^- - u_0, \varphi(0)^- \right\rangle \tag{3.21}$$

$$\rho^*(z_{kh})(\psi) := \mathcal{J}'(u_{kh})(\psi) - A^*(z_{kh})(\psi) - \left\langle z_{kh,M}^-, \psi(T)^- \right\rangle \tag{3.22}$$

for arbitrary $\varphi \in \mathcal{Y}$ and $\psi \in \mathcal{X} + \mathcal{X}_{kh}^{r,p}$.

Theorem 3.3. *Suppose that $\{u, z\} \in \mathcal{X} \times \mathcal{Y}$ is a stationary point of the Lagrangian functional $\mathcal{L}$ defined in* (3.12) *such that* (3.14) *is satisfied. Let $\{u_{kh}, z_{kh}\} \in \mathcal{X}_{kh}^{r,p} \times \mathcal{X}_{kh}^{r,p}$ denote its Galerkin approximation being defined by* (3.9) *and* (3.10) *such that* (3.15) *is satisfied. Then there holds the error representation that*

$$\mathcal{J}(u) - \mathcal{J}(u_{kh}) = \frac{1}{2}\rho(u_{kh})(z - \varphi_{kh}) + \frac{1}{2}\rho^*(z_{kh})(u - \psi_{kh}) + \mathcal{R}_{\mathcal{S}} + \mathcal{R}_{\mathcal{J}} \tag{3.23}$$

for arbitrary functions $\{\varphi_{kh}, \psi_{kh}\} \in \mathcal{X}_{kh}^{r,p} \times \mathcal{X}_{kh}^{r,p}$, where the remainder terms are defined by

$$\mathcal{R}_{\mathcal{S}} := \frac{1}{2}S(u_{kh})(\varphi_{kh} + z_{kh}) + \frac{1}{2}S^*(z_{kh})(\psi_{kh} - u_{kh}) + \sum_{m=0}^{M-1} \langle [z_{kh}]_m, [\psi_{kh} - u_{kh}]_m \rangle \tag{3.24}$$

and

$$\mathcal{R}_{\mathcal{J}} := \frac{1}{2}\int_0^1 \mathcal{J}'''(u_{kh} + s \cdot e)(e, e, e) \cdot s \cdot (s - 1)\, \mathrm{d}s \tag{3.25}$$

with $e = u - u_{kh}$.

Proof. Let $x := \{u, z\}$ with $\{u, z\} \in \mathcal{X} \times \mathcal{Y}$ be a stationary point of $\mathcal{L}$ in (3.12) such that (3.14) is satisfied. Let $x_{kh} := \{u_{kh}, z_{kh}\}$ with $\{u_{kh}, z_{kh}\} \in \mathcal{X}_{kh}^{r,p} \times \mathcal{X}_{kh}^{r,p}$ denote the Galerkin approximation of x that is defined by (3.9) and (3.10), respectively. From (3.12) along with (3.14) and (3.9) we conclude that

$$\mathcal{J}(u) - \mathcal{J}(u_{kh}) = \mathcal{L}(x) - \mathcal{L}(x_{kh}) + S(u_{kh})(z_{kh})\,.$$

As mentioned above, condition (3.18) is satisfied in our case. By Thm. 3.2 we get that

$$\mathcal{J}(u) - \mathcal{J}(u_{kh}) = \frac{1}{2}\mathcal{L}'(x_{kh})(x - y_{kh}) + \frac{1}{2}\mathcal{D}(x_{kh})(y_{kh} - x_{kh}) + S(u_{kh})(z_{kh}) + \mathcal{R} \tag{3.26}$$

for all $y_{kh} = \{\psi_{kh}, \varphi_{kh}\} \in \mathcal{X}_{kh}^{r,p} \times \mathcal{X}_{kh}^{r,p}$ with the remainder $\mathcal{R}$ being defined by (3.20). Recalling the definition (3.12) of $\mathcal{L}$ yields for the remainder $\mathcal{R}$ the asserted representation (3.25).

Next, from (3.13) along with the definitions (2.11) and (3.11) it follows that

$$\begin{aligned}
&\mathcal{L}'(u_{kh}, z_{kh})(u - \psi_{kh}, z - \varphi_{kh}) \\
&= \mathcal{J}'(u_{kh})(u - \psi_{kh}) - A^*(z_{kh})(u - \psi_{kh}) - \left\langle z_{kh,M}^-, u(T) - \psi_{kh,M}^- \right\rangle \\
&\qquad + F(z - \varphi_{kh}) - A(u_{kh})(z - \varphi_{kh}) - \left\langle u_{kh,0}^- - u(0), z(0) - \varphi_{kh,0}^- \right\rangle \\
&= \rho^*(z_{kh})(u - \psi_{kh}) + \rho(u_{kh})(z - \varphi_{kh})
\end{aligned}$$

for all $\{\psi_{kh}, \varphi_{kh}\} \in \mathcal{X}_{kh}^{r,p} \times \mathcal{X}_{kh}^{r,p}$. Substituting this identity into (3.26) yields that

$$\begin{aligned}
\mathcal{J}(u) - \mathcal{J}(u_{kh}) = \frac{1}{2}\rho^*(z_{kh})(u - \psi_{kh}) + \frac{1}{2}\rho(u_{kh})(z - \varphi_{kh}) \\
+ \frac{1}{2}\mathcal{D}(x_{kh})(y_{kh} - x_{kh}) + S(u_{kh})(z_{kh}) + \mathcal{R}\,.
\end{aligned} \tag{3.27}$$

Finally, we note that

$$\begin{aligned}
&\frac{1}{2}\mathcal{D}(x_{kh})(y_{kh} - x_{kh}) + S(u_{kh})(z_{kh}) \\
&= \frac{1}{2}S(u_{kh})(\varphi_{kh} - z_{kh}) + \frac{1}{2}S^*(z_{kh})(\psi_{kh} - u_{kh}) \\
&\qquad + \sum_{m=0}^{M-1} \langle [z_{kh}]_m, [\psi_{kh} - u_{kh}]_m \rangle + S(u_{kh})(z_{kh}) \\
&= \frac{1}{2}S(u_{kh})(\varphi_{kh} + z_{kh}) + \frac{1}{2}S^*(z_{kh})(\psi_{kh} - u_{kh}) \\
&\qquad + \sum_{m=0}^{M-1} \langle [z_{kh}]_m, [\psi_{kh} - u_{kh}]_m \rangle\,.
\end{aligned} \tag{3.28}$$

Combining (3.27) with (3.28) proves the assertion of the theorem. □

In the error respresentation (3.23) the continuous solution u or some higher order approximation of u is required for the evaluation of the adjoint residual. In the following theorem we show that the adjoint residual coincides with the primal residual up to a quadratic remainder. This observation will be exploited below to find our final error respresentation in terms of the goal quantity J and a suitable linearization for its computational evaluation or approximation, respectively.

Theorem 3.4. *Suppose that $\{u, z\} \in \mathcal{X} \times \mathcal{Y}$ is a stationary point of the Lagrangian functional $\mathcal{L}$ defined in* (3.12) *such that* (3.14) *is satisfied. Let $\{u_{kh}, z_{kh}\} \in \mathcal{X}_{kh}^{r,p} \times \mathcal{X}_{kh}^{r,p}$*

denote its Galerkin approximation being defined by (3.9) *and* (3.10) *such that* (3.15) *is satisfied. Let the primal and adjoint residuals be defined by* (3.21), (3.22). *Then there holds that*

$$\begin{aligned}\rho^*(z_{kh})(u-\psi_{kh}) = \rho(u_{kh})(z-\varphi_{kh}) + S(u_{kh})(\varphi_{kh}-z_{kh}) \\ + S^*(z_{kh})(u_{kh}-\psi_{kh}) + \Delta\rho_{\mathcal{J}}\end{aligned} \tag{3.29}$$

for all $\{\psi_{kh},\varphi_{kh}\} \in \mathcal{X}_{kh}^{r,p} \times \mathcal{X}_{kh}^{r,p}$ *with the remainder term*

$$\Delta\rho_{\mathcal{J}} := -\int_0^1 J''(u_{kh}+s\cdot e)(e,e)\,\mathrm{d}s \tag{3.30}$$

with $e := u - u_{kh}$.

Proof. Let $e := u - u_{kh}$ and $e^* := z - z_{kh}$ denote the primal and adjoint error, respectively. For arbitrary $\psi_{kh} \in \mathcal{X}_{kh}^{r,p}$ we put

$$\begin{aligned}k(s) := \mathcal{J}'(u_{kh}+s\cdot e)(u-\psi_{kh}) - A^*(z_{kh}+s\cdot e^*)(u-\psi_{kh}) \\ - \left\langle z_{kh,M}^- + s\cdot e_M^{*,-}, u(T) - \psi_{kh,M}^- \right\rangle .\end{aligned}$$

We have that

$$k(1) := \mathcal{J}'(u)(u-\psi_{kh}) - A^*(z)(u-\psi_{kh}) - \left\langle z(T), u(T)-\psi_{kh,M}^- \right\rangle = 0\,.$$

From (3.22) we get that

$$\begin{aligned}k(0) &= \mathcal{J}'(u_{kh})(u-\psi_{kh}) - A^*(z_{kh})(u-\psi_{kh}) - \left\langle z_{kh,M}^-, u(T)-\psi_{kh,M}^- \right\rangle \\ &= \rho^*(z_{kh})(u-\psi_{kh})\,.\end{aligned}$$

Further, we conclude that

$$\begin{aligned}k'(s) = \mathcal{J}''(u_{kh}+s\cdot e)(e,u-\psi_{kh}) - A^*(e^*)(u-\psi_{kh}) \\ - \left\langle e_M^{*,-}, u(T)-\psi_{kh,M}^- \right\rangle .\end{aligned}$$

Using (3.10) and (3.22) we find that

$$\begin{aligned}\rho^*(z_{kh})(u-\psi_{kh}) &= \mathcal{J}'(u_{kh})(u-\psi_{kh}) - A^*(z_{kh})(u-\psi_{kh}) \\ &\quad - \left\langle z_{kh,M}^-, u(T)-\psi_{kh,M}^- \right\rangle + S^*(z_{kh})(\psi_{kh}) - S^*(z_{kh})(\psi_{kh}) \\ &\quad - \mathcal{J}'(u_{kh})(u_{kh}) + A^*(z_{kh})(u_{kh}) + S^*(z_{kh})(u_{kh}) + \left\langle z_{kh,M}^-, u_{kh,M}^- \right\rangle \\ &= \rho^*(z_{kh})(u-u_{kh}) + S^*(z_{kh})(u_{kh}-\psi_{kh}) \\ &= \rho^*(z_{kh})(e) + S^*(z_{kh})(u_{kh}-\psi_{kh})\,.\end{aligned} \tag{3.31}$$

From (3.31) along with the theorem of calculus $\int_0^1 k'(s)\,\mathrm{d}s = k(1) - k(0)$ it follows that

$$\begin{aligned}
\rho^*(z_{kh})(u - \psi_{kh}) &= \rho^*(z_{kh})(e) + S^*(z_{kh})(u_{kh} - \psi_{kh}) \\
&= k(0) - k(1) + S^*(z_{kh})(u_{kh} - \psi_{kh}) \\
&= \int_0^1 \Big(A^*(e^*)(e) + \big\langle e_M^{*,-}, e_M^- \big\rangle - J''(u_{kh} + s \cdot e)(e,e) \Big)\,\mathrm{d}s + S^*(z_{kh})(u_{kh} - \psi_{kh}) \\
&= A^*(e^*)(e) + \big\langle e_M^{*,-}, e_M^- \big\rangle + S^*(z_{kh})(u_{kh} - \psi_{kh}) + \Delta\rho_{\mathcal{J}}\,. \qquad (3.32)
\end{aligned}$$

Next, for the first and second of the terms on the right-hand side of (3.32) we get that

$$\begin{aligned}
A^*(e^*)(e) + \big\langle e_M^{*,-}, e_M^- \big\rangle &= \sum_{m=1}^{M} - \int_{I_m} \langle \partial_t e^*, e \rangle\,\mathrm{d}t - \langle\langle b \cdot \nabla e^*, e \rangle\rangle + \langle\langle \varepsilon \nabla e^*, \nabla e \rangle\rangle \\
&\quad + \langle\langle \alpha e^*, e \rangle\rangle - \sum_{m=0}^{M-1} \big\langle [e^*]_m\,, e_m^+ \big\rangle + \big\langle e_M^{*,-}, e_M^- \big\rangle \\
&= \sum_{m=1}^{M} \int_{I_m} \langle \partial_t e, e^* \rangle\,\mathrm{d}t + \langle\langle b \cdot \nabla e, e^* \rangle\rangle + \langle\langle \varepsilon \nabla e, \nabla e^* \rangle\rangle \\
&\quad + \langle\langle \alpha e, e^* \rangle\rangle + \sum_{m=0}^{M-1} \big\langle [e]_m\,, e_m^{*,-} \big\rangle + \big\langle e_0^-, e_0^{*,-} \big\rangle \\
&= F(e^*) + \big\langle u_0, e_0^{*,-} \big\rangle - A(u_{kh})(e^*) - \Big\langle u_{kh,0}^-, e_0^{*,-} \Big\rangle \\
&= \rho(u_{kh})(z - z_{kh}) = \rho(u_{kh})(z - \varphi_{kh}) + S(u_{kh})(\varphi_{kh} - z_{kh}) \qquad (3.33)
\end{aligned}$$

for all $\varphi_{kh} \in \mathcal{X}_{kh}^{r,p}$. Combining (3.32) with (3.33) yields that

$$\begin{aligned}
\rho^*(z_{kh})(u - \psi_{kh}) &= \rho(u_{kh})(z - \varphi_{kh}) + S(u_{kh})(\varphi_{kh} - z_{kh}) \\
&\quad + S^*(z_{kh})(u_{kh} - \psi_{kh}) + \Delta\rho_{\mathcal{J}}
\end{aligned}$$

for all $\{\psi_{kh}, \varphi_{kh}\} \in \mathcal{X}_{kh}^{r,p} \times \mathcal{X}_{kh}^{r,p}$ with $\Delta\rho_{\mathcal{J}}$ being defined by (3.30). This proves the assertion of the theorem. □

We summarize the results of the previous two theorems in the following corollary.

Corollary 3.5. *Suppose that $\{u, z\} \in \mathcal{X} \times \mathcal{Y}$ is a stationary point of the Lagrangian finctional $\mathcal{L}$ defined in* (3.12) *such that* (3.14) *is satisfied. Let $\{u_{kh}, z_{kh}\} \in \mathcal{X}_{kh}^{r,p} \times \mathcal{X}_{kh}^{r,p}$ denote its Galerkin approximation being defined by* (3.9) *and* (3.10) *such that* (3.15) *is satisfied. Then there holds the error representation that*

$$\mathcal{J}(u) - \mathcal{J}(u_{kh}) = \rho(u_{kh})(z - \varphi_{kh}) + \mathcal{R}_{\mathcal{S}} + \mathcal{R}_{\mathcal{J}} + \frac{1}{2}\Delta\rho_{\mathcal{J}} \qquad (3.34)$$

for arbitrary functions $\varphi_{kh} \in \mathcal{X}_{kh}^{r,p}$*, where the primal residual* $\rho(u_{kh})(\cdot)$ *is defined by* (3.21)*, the remainder term* $\mathcal{R}_{\mathcal{J}}$ *is given by* (3.25)*, the linearization error* $\Delta\rho_{\mathcal{J}}$ *is defined by* (3.30) *and*

$$\mathcal{R}_{\mathcal{S}} := S(u_{kh})(\varphi_{kh}) + \sum_{m=0}^{M-1} \langle [z_{kh}]_m, [\psi_{kh} - u_{kh}]_m \rangle \tag{3.35}$$

for arbitrary functions $\psi_{kh} \in \mathcal{X}_{kh}^{r,p}$*.*

We note that the notation $\mathcal{R}_{\mathcal{S}}$ in (3.35) is used generically and defined differently in different equations of its occurence. In the final step of deriving an a posteriori error representation we give a localized error approximation that can used to design an adaptive algorithm.

Theorem 3.6 (Localized error representation)**.** *Suppose that* $\{u, z\} \in \mathcal{X} \times \mathcal{Y}$ *is a stationary point of the Lagrangian functional* $\mathcal{L}$ *defined in* (3.12) *such that* (3.14) *is satisfied. Let* $\{u_{kh}, z_{kh}\} \in \mathcal{X}_{kh}^{r,p} \times \mathcal{X}_{kh}^{r,p}$ *denote its Galerkin approximation being defined by* (3.9) *and* (3.10) *such that* (3.15) *is satisfied. Neglecting the higher order error terms in* (3.34)*, then there holds as a linear approximation the cell-wise error representation*

$$\begin{aligned}
\mathcal{J}(u) - \mathcal{J}(u_{kh}) \doteq \int_0^T \sum_{K\in\mathcal{T}_h} \Big\{ & \langle \mathcal{R}(u_{kh}), z - \varphi_{kh} \rangle_{\mathcal{L}^2(K)} - \delta_K \langle \mathcal{R}(u_{kh}), \boldsymbol{b}\cdot\nabla\varphi_{kh} \rangle_{\mathcal{L}^2(K)} \\
& - \langle \mathcal{E}(u_{kh}), z - \varphi_{kh} \rangle_{\partial K} \Big\} \,\mathrm{d}t - \left\langle u_{kh,0}^- - u_0, z(t_0) - \varphi_{kh,0}^- \right\rangle_{\mathcal{L}^2(\Omega)} \\
& - \sum_{m=0}^{M-1} \left\langle [u_{kh}]_m \,, z(t_m) - \varphi_{kh,m}^+ \right\rangle_{\mathcal{L}^2(\Omega)} \\
& + \sum_{K\in\mathcal{T}_h} \delta_K \left\langle u_{kh,0}^- - u_0, \boldsymbol{b}\cdot\nabla\varphi_{kh,0}^- \right\rangle_{\mathcal{L}^2(K)} \\
& + \sum_{m=0}^{M-1} \sum_{K\in\mathcal{T}_h} \delta_K \left\langle [u_{kh}]_m \,, \boldsymbol{b}\cdot\nabla\varphi_{kh,m}^+ \right\rangle_{\mathcal{L}^2(K)} .
\end{aligned} \tag{3.36}$$

The cell- and edge-wise residuals are defined by

$$\mathcal{R}(u_{kh})_{|K} := f - \partial_t u_{kh} - \boldsymbol{b}\cdot\nabla u_{kh} + \nabla\cdot(\varepsilon\nabla u_{kh}) - \alpha u_{kh} \,, \tag{3.37}$$

$$\mathcal{E}(u_{kh})_{|\Gamma} := \begin{cases} \frac{1}{2}\boldsymbol{n}\cdot[\varepsilon\nabla u_{kh}] & \text{if } \Gamma \subset \partial K \backslash \partial\Omega \,, \\ 0 & \text{if } \Gamma \subset \partial\Omega \,, \end{cases} \tag{3.38}$$

where $[\nabla u_{kh}] := \nabla u_{kh|\Gamma\cap K'} - \nabla u_{kh|\Gamma\cap K}$ *defines the jump of* ∇u_{kh} *over the inner edges* Γ *with normal unit vector* $\boldsymbol{n}$ *pointing from* K' *to* K*.*

Proof. The assertion directly follows from (3.34), (3.35) by neglecting the higher order remainder terms $\mathcal{R}_{\mathcal{J}}$ and $\Delta\rho_{\mathcal{J}}$, choosing $\psi_{kh} = u_{kh}$ in (3.35) and applying integration by parts on each cell $K \in \mathcal{T}_h$ to the diffusive term in the primal residual (3.21). □

Finally, we summarize the result of our application of the DWR approach to the stabilized approximation (2.18)–(2.20) of the nonlinear stationary problem (2.17). In terms of a *first dualize and then stabilize* philosophy analogously to (3.10) we get that

$$\mathcal{J}(u) - \mathcal{J}(u_h) = \rho(u_h)(z - \varphi_h) + \mathcal{R}_{\mathcal{S}} + \mathcal{R}_{\mathrm{nl}} + \frac{1}{2}\Delta\rho_{\mathcal{S}} + \frac{1}{2}\Delta\rho_{\mathrm{nl}} \tag{3.39}$$

with the primal residual

$$\rho(u_h)(\varphi) := F(\varphi) - A(u_h)(\varphi) \tag{3.40}$$

and the remainder terms of the stabilization

$$\mathcal{R}_{\mathcal{S}} + \frac{1}{2}\Delta\rho_{\mathcal{S}} = S(u_h)(\varphi_h) + S_C(u_h)(\varphi_h) \tag{3.41}$$

as well as the higher order remainder terms

$$\begin{aligned}\mathcal{R}_{\mathrm{nl}} := \frac{1}{2}\int_0^1 \Big\{ &\mathcal{J}'''(u_h + se)(e,e,e) - \big\langle r'''(u_h + se)e^3, z_h + se^* \big\rangle \\ &-3\left\langle r''(u_h + se)e^2, e^* \right\rangle_\Omega \Big\} \cdot s \cdot (s-1)\,\mathrm{d}s\,,\end{aligned} \tag{3.42}$$

$$\Delta\rho_{\mathrm{nl}} = S(u_h)(\varphi_h - z_h) + S_C(u_h)(\varphi_h - z_h) - S^*(u_h)(\zeta_h - u_h, z_h)\,. \tag{3.43}$$

The forms arising in (3.40) to (3.43) are defined in (2.19). We denote by $e := u - u_h$ and $e^* := z - z_h$ the approximation error of the primal and adjoint problem, respectively. For a proof of (3.39) we refer to [46]. In [46], the *first stabilize and then dualize* approach to stationary convection-dominated problems is further presented, investigated numerically and compared with the error representation (3.39). Finally, neglecting the higher order remainder terms $\mathcal{R}_{\mathrm{nl}}$ and $\Delta\rho_{\mathrm{nl}}$ defined in (3.42) and (3.43), respectively, and using integration by parts we derive from (3.39) the linearized cell-wise error representation (cf. [46])

$$\begin{aligned}\mathcal{J}(u) - \mathcal{J}(u_h) \doteq \sum_{K\in\mathcal{T}_h} \Big\{ &\langle \mathcal{R}(u_h), z - \varphi_h\rangle_K - \delta_K \langle \mathcal{R}(u_h), \boldsymbol{b}\cdot\nabla\varphi_h\rangle_K \\ &+ S_C(u_h)(\varphi_h) - \langle \mathcal{E}(u_h), z - \varphi_h\rangle_{\partial K} \Big\}\,.\end{aligned} \tag{3.44}$$

The cell and edge residuals are defined analogously to (3.37), (3.38) by

$$\mathcal{R}(u_h)_{|K} = f + \nabla\cdot(\varepsilon\nabla u_h) - \boldsymbol{b}\cdot\nabla u_h - \alpha u_h - r(u_h)\,, \tag{3.45}$$

$$\mathcal{E}(u_h)_{|\Gamma} = \begin{cases} \frac{1}{2}\boldsymbol{n}\cdot[\varepsilon\nabla u_h]\,, & \text{if } \Gamma \subset \partial K\backslash\partial\Omega\,, \\ 0\,, & \text{if } \Gamma \subset \partial\Omega\,. \end{cases} \tag{3.46}$$

4. Practical Aspects

In this section we discuss some aspects of the practical use of the DWR approach presented in Section 3 for the numerical approximation of convection-dominated problems. The error representation (3.36), written in the form

$$\mathcal{J}(u) - \mathcal{J}(u_{kh}) \doteq \eta := \sum_{m=1}^{M} \sum_{K \in \mathcal{T}_h} \eta_K^m \,, \tag{4.1}$$

depends on the discrete primal solution as well as on the exact dual solution z. For solving the primal problem (2.1) we use the discontinuous in time scheme (2.15) and compute a discrete solution $u_{kh} \in \mathcal{X}_{kh}^{r,p}$. As mentioned in Section 1 and shown by (3.35) and (3.36), respectively, the approximation of the dual solution cannot be done in the finite element space of the primal problem since it would result in a vanishing primal residual $\rho(u_{kh})(\cdot)$. For the approximation of the dual solution z we use the SUPG stabilized counterpart of the continuous in time scheme (2.14) and compute a discrete approximation $z_{kh} \in \overline{\mathcal{X}}_{kh}^{r+1,p+1}$.

In contrast to many other works of the literature we thus use a higher order approach, i.e. $z_{kh} \in \overline{\mathcal{X}}_{kh}^{r+1,p+1}$, compared with the primal problem for the approximation of the dual solution which leads to higher computational costs; cf. [7, 35] for algorithmic formulations and analyses. In the literature the application of a higher order interpolation is often suggested for the DWR approach; cf. [3, 4]. For convection-dominated problems such an interpolation might be defective and lead to tremendous errors close to sharp layers and fronts. Higher order techniques show more stability and reduce spurious oscillations (cf. [8]) which is our motivation for using a higher order approximation of the dual solution. For nonlinear problems the additional costs for computing the higher order approximation of the dual solution are moderate, since the adjoint problem is always a linear one and, thereby, does not require nonlinear (e.g. Newton) iterations for solving the discrete problem whereas such iterations become necessary in the nonlinear case for the primal problem.

In order to define the localized error contributions η_K^m in (4.1) we consider a hierarchy of sequentially refined meshes $\mathcal{M}_i^m$, with $i \geq 1$ indexing the hierarchy and m indexing the subintervals or time steps, respectively. The initial mesh $\mathcal{M}_0^m$ is identical for each time step m, i.e. $M_0^i = M_0^j$ for all $i, j = \{1, \ldots, M\}$. The corresponding finite element spaces are denoted by $\mathcal{V}_h^{p+1,m,i}$ (cf. (2.12)) with the additional index i denoting the mesh hierarchy. We calculate the cell- and step-wise contributions to the linearized

error representation (4.1) and (3.36), respectively, by means of

$$\begin{aligned}\eta_K^m = \int_{I_m} & \langle \mathcal{R}(u_h^{m,i}, z_H^{m,i} - \mathcal{I}_h z_H^{m,i}\rangle_K - \delta_K \langle \mathcal{R}(u_h^{m,i}, \boldsymbol{b}\cdot\nabla \mathcal{I}_h z_H^{m,i}\rangle_K \\ & - \langle \mathcal{E}(u_h^{m,i}), z_H^{m,i} - \mathcal{I}_h z_H^{m,i}\rangle_{\partial K}\, dt - \left\langle \left[u_h^i\right]_{m-1}, z_H^{m-1,i} - \mathcal{I}_h z_H^{m-1,i}\right\rangle_\Omega \\ & + \delta_K \left\langle \left[u_h^i\right]_{m-1}, \boldsymbol{b}\cdot\nabla I_h z_H^{m-1,i}\right\rangle_K ,\end{aligned} \tag{4.2}$$

where the cell and edge residuals are given in (3.37) and (3.38), respectively, and $\left[u_h^i\right]_0 := u_h^{1,i} - u_0$. By $I_h z_H^{m,i} \in \mathcal{V}_h^{p,m,i}$ we denote the linear interpolation of the higher order approximation $z_H^{m,i} \in \mathcal{V}_h^{p+1,m,i}$. The integrals over the time intervals I_m are approximated by an appropriate quadrature rule depending on the polynomial degree of the time discretization. For a discussion of appropriate mesh refinement strategies we refer to, e.g., [3]. Details about the refinement strategy in time and in space that we use for the computations that are presented in Section 5 can be found in [46]. In the steady case an approach that is analogous to (4.2) is used.

For the numerical computations of Section 5 we used the lowest order variants of the discretization schemes for the approximation of the primal and the dual solution. The discrete primal problem (2.15) is thus solved in the function space $\mathcal{X}_{kh}^{0,1}$. Up to a quadrature error in the right-hand side term f the scheme is then algebraically equivalent to a backward Euler scheme in time with piecewise linear polynomials in space; cf. [45] and the reference therein. The adjoint problem is then solved by the SUPG stabilized counterpart of the scheme (2.14) and yields a discrete solution $z_H^i \in \overline{\mathcal{X}}_{kh}^{1,2}$ being continuous and piecewise linear and continuous and piecewise quadratic in space. Up to a quadrature error in the right hand side this scheme is algebraically equivalent to the Crank-Nicolson approach [4, 45].

For measuring the accuracy of the error estimators we will use the effectivity index

$$\mathcal{I}_{eff} = \left| \frac{\eta}{\mathcal{J}(u) - \mathcal{J}(u_{kh})} \right| , \tag{4.3}$$

as the ratio of the estimated error η of (4.1) over the exact error. Desirably, $\mathcal{I}_{eff}$ should be close to one. In the steady case $\mathcal{I}_{eff}$ is defined analogously with u_{kh} being substituted by u_h.

5. Numerical studies

In this section we illustrate and investigate the performance properties of the proposed approach of applying the dual weighted residual method to stabilized finite element approximations of convection-dominated problems.

Example 1 (Hump with changing height). As a test setting we study the moving hump problem that has been used in several works [33, 8, 1] before as a benchmark

problem for approximation schemes to convection-dominated equations. We consider problem (2.1) with the prescribed solution

$$\begin{aligned} u(\boldsymbol{x},t) = \frac{16}{\pi}\sin(\pi t)x_1(1-x_1)x_2(1-x_2) \\ \cdot\left\{\frac{\pi}{2} + \arctan\left(2\varepsilon^{-\frac{1}{2}}(z_0^2 - (x_1-x_1^0)^2 - (x_2-x_2^0)^2)\right)\right\}, \end{aligned} \tag{5.1}$$

where $\Omega \times I := (0,1)^2 \times (0,0.5]$ and $z_0 = 0.25$, $x_1^0 = x_2^0 = 0.5$. For the final time $T = 0.5$ the hump reaches its maximum height. We choose the parameter $\varepsilon = 10^{-6}$, $\boldsymbol{b} = (2,3)^\top$ and $\alpha = 1.0$. For the solution (5.1) the right-hand side function f is calculated from the partial differential equation. Boundary and initial conditions are given by the exact solution. Our target quantity is chosen as

$$\mathcal{J}(u) = \int_\Omega u(\boldsymbol{x},T)\,\mathrm{d}\boldsymbol{x}\,. \tag{5.2}$$

We measure the spurious oscillations of the solution in the layer around the hump by

$$\mathrm{var}(t) := \max_{\boldsymbol{x}\in\Omega} u_{kh}(\boldsymbol{x},t) - \min_{\boldsymbol{x}\in\Omega} u_{kh}(\boldsymbol{x},t)\,, \tag{5.3}$$

where the maximum and minimum are taken only in the vertices of the mesh cells. The exact value for the function u of (5.1) at $t = 0.5$ is $\mathrm{var}(0.5) = 0.997453575$; cf. [33].

Our SUPG-stabilized discretization scheme (2.15) for the primal problem is applied with the lowest order parameter choice which amounts to $r = 0$ and $p = 1$. The dG(0) variational time discretization thus coincides with the backward Euler approach. For the discretization in space piecewise polynomials of first order degree are thus chosen. According to our derivation in Section 3 we use a higher order approach with $r = 1$ and $p = 2$ for the discretization of the adjoint problem .

In Figure 5.1 we visualize our computed solution profiles for the time points $t = 0.25$ and $t = 0.5$ after 16 DWR iterations on the whole time interval $(0,T]$. For $t = 0.25$ the solution is still strongly perturbed in the backward part of the hump's layer and behind the hump in the direction of the flow field $\boldsymbol{b}$. The mesh is coarse in that part of the domain. Such a behaviour is admissible since our target functional aims to control the solution profile at the final time point $T = 0.5$ only. For $T = 0.5$ an almost perfect solution profile is obtained and the finite element mesh cells are concentrated on the backward face of the hump. We note that the spurious oscillations behind the hump, that were obtained by different classes of approximation schemes in [33], do not arise here. They are strongly reduced and almost completely eliminated by the adaptive algorithm. In Figure 5.2 the magnitude of the adaptively chosen time steps is presented. The first time steps are chosen relatively large whereas the time step sizes close to the final time point $T = 0.5$ become much smaller. Even though large time step sizes and also large spatial mesh sizes in the crucial regions are used in the first time steps, leading to crude approximations in the initial phase as shown in the left plot of Figure 5.1, the algorithm is capable to provide the desired approximation

quality in the target quantity (5.2) that is local in time and controls the solution profile at the time final time point only. A high approximation quality in the target quantity is thus obtained with very economical meshes.

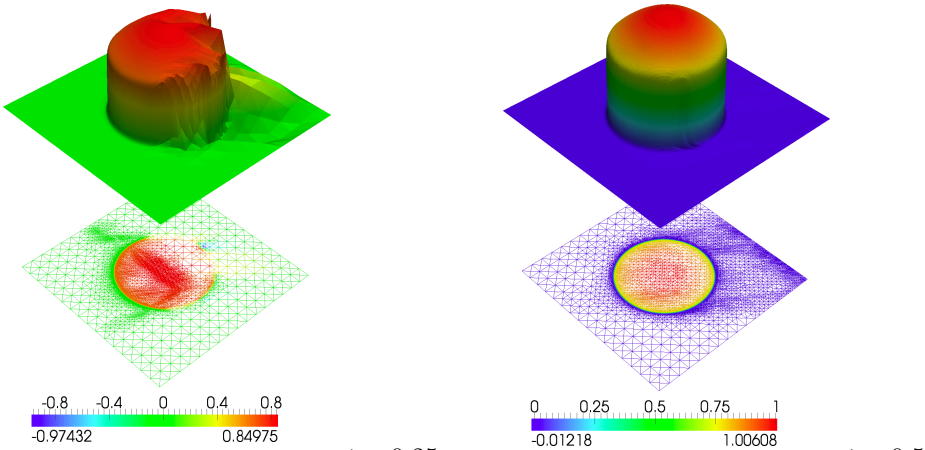

Figure 5.1: Solution and adaptive mesh for goal quantity (5.2) at time $t = 0.25$ (*left*) and at time $t = 0.5$ (*right*) for Example 1.

In Table 5.2 we monitor the convergence behaviour of the DWR iterations in terms of the effectivity index (4.3) for the target functional (5.2). The degrees of freedom at the final time point $T = 0.5$ are given together with the corresponding values of the effectivity index and var(0.5). For an increasing number of DWR iterations with space-time mesh adaptions the effectivity index is very close to one indicating an excellent approximation of the goal quantity by the DWR approach applied to the stabilized approximation of (2.1). Further, the given numbers for var(0.5) show that the spurious oscillations in the layer around the hump are also reduced by the DWR iterations and the space-time grid adaption process. This might be a consequence of the global character in space of the target functional (5.2). Finally in Table 5.1 we compare the values for var(0.5) that we computed by our adaptive approach with some reference values that were obtained by other research groups and published in the literature. The calculations of all other groups were done on uniform meshes. For comparison purposes our adaptive simulations were run in such a way that either the number of degrees or the calculated value var(0.5) coincides approximately with the given reference values of the literature. The presented numbers impressively illustrate the superiority of the adaptive computations.

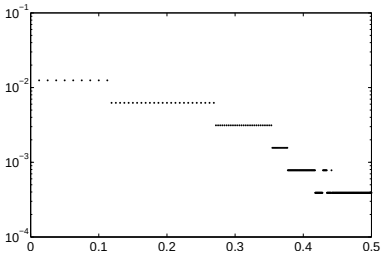

Figure 5.2: Time step sizes over $(0, T]$ for Example 1.

dofs	var(0.5)	$\mathcal{I}_{eff}$	dofs	var(0.5)	$\mathcal{I}_{eff}$
545	9.392	1.03	6425	1.200	1.02
833	9.432	1.17	7283	1.115	1.00
1267	5.852	1.75	8939	1.076	0.96
1535	6.761	9.13	11954	1.079	0.97
2325	4.328	2.82	20757	1.050	0.99
2522	3.270	1.08	21455	1.030	1.03
3031	2.105	1.47	25492	1.022	1.05
3937	1.568	0.94	36167	1.018	1.07

Table 5.1: Convergence statistics for Example 1.

Method	Reference	var(0.5)	dofs	k
SUPG	[33]	1.3835	16641	10^{-3}
LPS	[33]	1.2007	32768	10^{-3}
SUPG	[8]	1.2504	33025	$2 \cdot 10^{-3}$
SUPG/SC	[8]	1.1946	33025	$2 \cdot 10^{-3}$
LPS/cGP(1)	[1]	1.0408	33025	10^{-3}
LPS/dG(1)	[1]	1.0408	33025	10^{-3}
SUPG/DWR	this work	1.0790	10900	$3.1 \cdot 10^{-3}$
SUPG/DWR	this work	1.0179	35931	$1.5 \cdot 10^{-3}$

Table 5.2: Reference values of the literature for Example 1.

Example 2 (Point value error control). In this example we illustrate the application of our approach to a target functional that provides a spatially local error control in a sharp layer. Thereby we evaluate the potential of our approach to capture sharp layers and fronts with high accuracy. This is a challenging task and of utmost interest for convection-dominated problems. Since the interaction of the goal-oriented error control mechanism with the discretization in space is especially focused here, we restrict ourselves to the stationary case for simplicity. As a benchmark problem we use an adaptation of [37, Example 4.2]. We consider problem (2.17) with $\Omega = (0,1)^2$, $\alpha = 1.0$, $\boldsymbol{b} = \frac{1}{\sqrt{5}}(1,2)^\top$, $\varepsilon = 10^{-6}$ and nonlinear reaction term $r(u) = u^2$. We choose the right-hand side f such that

$$u(\boldsymbol{x}) = \frac{1}{2}\left(1 - \tanh\frac{2x_1 - x_2 - 0.25}{\sqrt{5\varepsilon}}\right) \tag{5.4}$$

is the analytical solution of (2.17). The Dirichlet boundary condition is given by the exact solution. The solution is characterized by an interior layer of thickness $\mathcal{O}(\sqrt{\varepsilon}|\ln\varepsilon|)$. We study the following target functionals

$$\mathcal{J}_{\mathcal{L}^2}(u) = \frac{1}{\|e\|_{\mathcal{L}^2(\Omega)}}\langle e, u\rangle_\Omega\,, \qquad \mathcal{J}_1(u) = \int_\Omega u\,\mathrm{d}\boldsymbol{x} \qquad \text{and} \qquad \mathcal{J}_2(u) = u(\boldsymbol{x}_e)\,,$$

where $e := u - u_h$ and with a user-prescribed control point $\boldsymbol{x}_e = \left(\frac{3}{16}, \frac{1}{8}\right)$ that is located in the interior of the layer. In our computations we regularize the functional $\mathcal{J}_2(u)$ by

$$\mathcal{J}_r(u) = \frac{1}{|B_r|} \int_{B_r} u(\boldsymbol{x}) \, \mathrm{d}\boldsymbol{x} \,,$$

where the ball B_r is defined by $B_r = \{\boldsymbol{x} \in \Omega \,|\, |\boldsymbol{x} - \boldsymbol{x}_e| < r\}$ with a small radius r.

In Figure 5.3 and Table 5.3 we summarize the convergence behavior of proposed DWR approach to the stabilized approximation scheme (2.18). We note that $J_1(\cdot)$ provides the traditional global $\mathcal{L}^2$-error control and is considered for reference purposes. For the target functionals $\mathcal{J}_{\mathcal{L}^2}(\cdot)$ and $\mathcal{J}_1(\cdot)$ the effectivity indices converge to one for an increasing an number of degrees of freedom. For the challenging point value error control of $\mathcal{J}_r(\cdot)$ the effectivity index is also very close to one which is in good agreement with effectivity indices for point value error control that are given in other works of the literature; cf. [3, p. 45] for the pure Poisson problem. In Figure 5.4 we visualize the computed solution profiles and adaptive meshes for an error control based on the local target functional $\mathcal{J}_r$ and the global target functional $\mathcal{J}_1$, respectively. This example nicely brings out the potential of the DWR approach. For the point value error control the mesh cells are located around the specified point of interest. Even though a crude approximation of the sharp interface is obtained away from the specified control point, in its neighborhood an excellent approximation of the sharp layer is ensured by the approach. A very economical mesh along with a high quality in the computation of the user-specified goal quantity is thus obtained. The global error control of J_1 provides a good approximation of the solution in the whole domain by adjusting the mesh along the layer.

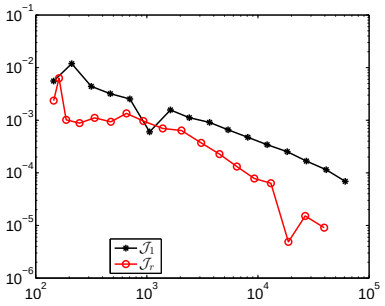

Figure 5.3: $\mathcal{J}_1(u - u_h)$ and $\mathcal{J}_r(u - u_h)$ over degrees of freedom for Example 2.

$\mathcal{J}_{\mathcal{L}^2}$		$\mathcal{J}_1$		$\mathcal{J}_r$	
dofs	$\mathcal{I}_{eff}$	dofs	$\mathcal{I}_{eff}$	$\mathcal{I}_{eff}$	dofs
3756	0.74	5383	0.45	0.03	4505
5903	0.83	8105	0.44	0.07	6458
9059	0.87	12081	0.45	0.14	9268
14373	0.94	18321	0.57	0.22	13079
22834	0.95	27276	0.71	3.42	18794
37555	0.97	41073	0.76	1.25	26619
62119	0.98	60957	0.83	2.27	39447

Table 5.3: Effectivity indices for the target quantities $\mathcal{J}_{\mathcal{L}^2}$, $\mathcal{J}_1$ and $\mathcal{J}_r$ for Example 2.

Example 3 (Impact of approximation of the weights). In the last example we briefly study the impact of the approximation of the dual solution z on the quality of the overall error control process. For brevity we consider again the test problem of Example 2 with the prescribed solution (5.4). In our first study we use a piecewise linear approximation in $\mathcal{V}_h^1$ with SUPG and additional shock-capturing stabilization for the

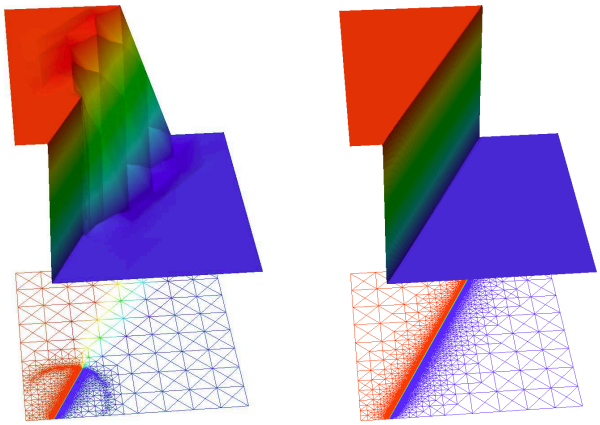

Point value error control. Global error control.

Figure 5.4: Point value error control (*left*) and global error control (*right*) by the DWR approach for Example 2.

primal problem. For the corresponding adjoint problem a piecewise quadratic finite approximation in $\mathcal{V}_h^2$ with SUPG stabilization and with and without additional shock-capturing stabilization is used. The left plot of Figure 5.5 shows that the additional shock-capturing stabilization of the dual problem yields no further improvement in the accuracy of the approximation. This is advantageous since the adjoint problem by itself is always a linear one. Applying shock-capturing stabilization introduces an artificial nonlinearity and requires (nonlinear) iterations for solving the arising algebraic system. The left plot of Figure 5.5 that argues that using only SUPG stabilization for the dual problem and thereby keeping its linear character is sufficient for the proposed DWR apporach. We note that the positive impact of additional shock-capturing stabilization in the numerical approximation of convection-dominated problems has been well understood and analyzed numerically; cf. [8, 33] and the references therein.

Further, the left plot of Figure 5.5 shows the gain in accuracy if a higher order approach is used. Here we combined a stabilized piecewise quadratic approximation in $\mathcal{V}_h^2$ of the primal problem with a stabilized approximation in $\mathcal{V}_h^4$ with piecewise polynomials of fourth order of the adjoint problem. An approximation of the adjoint problem with piecewise polynomials of third order did not provide sufficient accuracy and did not yield a convergence behaviour or an error reduction, respectively, similarly to the one that is shown in the left plot of Figure 5.5. This observation underlines the necessity of the proper approximation of the adjoint problem within the DWR framework. For non convection-dominated problems the process might be not that much sensitive as in our studies for problems with strong layers and sharp fronts. In the right plot of Figure 5.5 the corresponding values of the effectivity index are visualized.

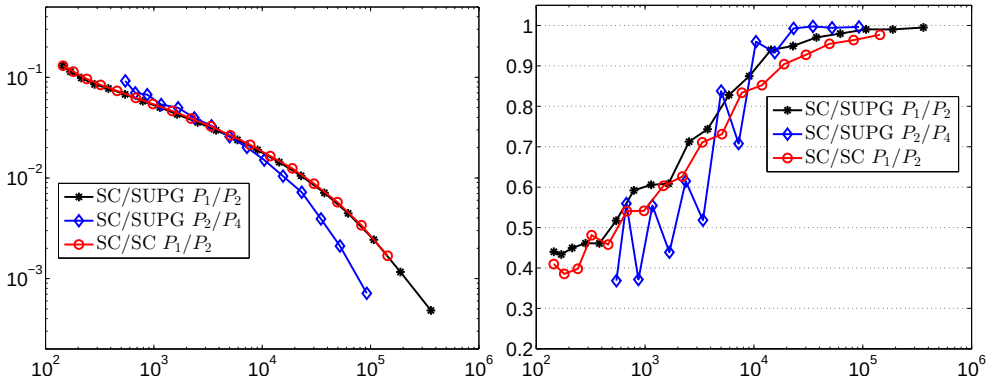

Figure 5.5: Errors $\mathcal{J}_{\mathcal{L}^2}(u - u_h)$ (*left*) and effectivity indices $\mathcal{I}_{\text{eff}}$ (*right*) over degrees of freedom for Example 3 with stabilization techniques for the primal/ dual problem and polynomial degrees for the approximation of the primal/ dual problem – SC indicates the application of additional shock–capturing stabilization, SUPG means SUPG stabilization only).

6. Summary

In this work we developed an adaptive approach for stabilized finite approximations of convection-dominated problems. It is based on the dual weighted residual method for goal-oriented a posteriori error control. A *first dualize and then stabilize* philosophy was applied for conmbing the dual weighted residual method with the stabilization of the finite element techniques. In contrast to other works of the literature we used a higher order approximation of the adjoint problem instead of a higher order interpolation of a lower order approximation of the dual solution. Thereby we aim to eliminate sources of inaccuracies in regions with layers and close to sharp fronts. In numerical experiments we could prove that spurious oscillations that typically arise in numerical approximations of convection-dominated problems could be reduced significantly. Effectivity indices very close to one were obtained for the user-specified target quantities. The presented approach offers large potential for combining goal-oriented error control and selfadaptivity with stabilized finite element methods in the approximation of convection-dominated transport. The application of the approach to more sophisticated problems, like Navier–Stokes problems, is our work for the future. Moreover, the efficient computation of the higher order approximation to the adjoint problem offers potential for optimization. This will also be our work for the future.

References

[1] N. Ahmed, G. Matthies, *Numerical studies of Galerkin-type time-discretizations applied to transient convection-diffusion-reaction equations*, World Acad. Sci. Eng. Tech., **66** (2012), pp. 586–593.

[2] R. Araya, P. Venegas, *An a posteriori error estimator for an unsteady advection-diffusion-reaction problem*, Comput. Math. Appl., **66** (2014), 2456–2476.

[3] W. Bangerth, R. Rannacher, *Adaptive Finite Element Methods for Differential Equations*, Birkhäuser, Basel, 2003.

[4] W. Bangerth, M. Geiger, R. Rannacher, *Adaptive Galerkin finite element methods for the wave equation*, Comput. Meth. Appl. Math., **10** (2010), pp. 3–48.

[5] M. Bause, P. Knaber, *Uniform error analysis for Lagrange–Galerkin approximations of convection-dominated problems*, SIAM J. Numer. Anal., **39** (2002), pp. 1954–1984.

[6] M. Bause, U. Köcher: *Iterative coupling of variational space-time methods for Biot's system of poroelasticity*, Prcoceedings of the ENUMATH 2015 Conference, **submitted** (2015), pp. 1–8.

[7] M. Bause, U. Köcher, *Variational time discretization for mixed finite element approximations of nonstationary diffusion problems*, J. Comput. Appl. Math., **289** (2015), pp. 208–224.

[8] M. Bause, K. Schwegler, *Analysis of stabilized higher order finite element approximation of nonstationary and nonlinear convection-diffusion-reaction equations*, Comput. Methods Appl. Mech. Engrg., **209–212** (2012), pp. 184–196.

[9] R. Becker, *An optimal-control approach to a posteriori error estimation for finite element discretizations of the Navier–Stokes equations*, East-West J. Numer. Math., **9** (2000), pp. 257–274.

[10] R. Bermejo, J. Carpio, *An adaptive finite element semi-Lagrangian implicit-explicit Runge-Kutta-Chebyshev method for convection dominated reaction-diffusion problems*, Appl. Numer. Math., **58** (2008), pp. 16–39.

[11] M. Braack, E. Burman, N. Taschenberger, *Duality based a posteriori error estimation for quasi periodic solutions using time averages*, SIAM J. Sci. Comput., **33** (2011), pp. 2199–2216.

[12] M. Braack, A. Ern, *A posteriori control of modeling errors and discretization errors*, SIAM J. Multiscale Modeling and Simulation, **1** (2003), pp. 221–238.

[13] M. Braak, T. Richter, *Solutions of 3D Navier–Stokes benchmark problems with adaptive finite elements*, Computers and Fluids, **35** (2006), pp. 372–392.

[14] E. Burmann, *A posteriori error estimation for interior penalty finite element approximations of advection-reaction equations*, SIMA J. Numer. Anal., **47** (2009), pp. 3584–3607.

[15] P. G. Ciarlet, *The Finite Element Methods for Elliptic Problems*, North–Holland, Amsterdam, 1978.

[16] R. Dautray, J.-L. Lions, *Mathematical Analysis and Numerical Methods for Science and Technology: Evolution Problems I, Vol. 5*, Springer, Berlin, 1992.

[17] V. Dolejší, A. Ern, M. Vohralík, *A framework for robust a posteriori error control in unsteady nonlinear advection-diffusion problems*, SIAM J. Numer. Anal., **51** (2013), pp. 773–793.

[18] K. Eriksson, C. Johanson, *Adaptive finite element methods for parabolic problems, I: a linear model problem*, SIAM J. Numer. Anal., **28** (1991), pp. 43–77.

[19] K. Eriksson, C. Johanson, *Adaptive finite element methods for parabolic problems, II: optimal error estimates in $L^\infty(L^2)$ and $L^\infty(L^\infty)$*, SIAM J. Numer. Anal., **32** (1995), pp. 706–740.

[20] L. C. Evans, *Partial Differential Equations*, American Mathematical Society, Providence, Rhode Island, 2010.

[21] J. de Frutos, B. García-Archilla, V. John, J. Novo, *An adaptive SUPG method for evolutionary convection dominated problems*, Comput. Methods Appl. Mech. Engrg., **200** (2011), pp. 3601–3612.

[22] J. de Frutos, B. García-Archilla, J. Novo, *Local error estimates for the SUPG method applied to evoluitionary convection-diffusion-reaction equations*, J. Sci. Comput., DOI 10.1007/s10915-015-0035-2 (2015), pp. 1–27.

[23] J. de Frutos, B. García-Archilla, V. John, J. Novo, *An adaptive SUPG method for evolutionary convection-diffusion equations*, Comput. Methods Appl. Mech. Engrg., **273** (2014), pp. 219–237.

[24] F. K. Hebeker, R. Rannacher, An adaptive finite element method for unsteady convection-dominated flows with stiff source term, SIAM J. Numer. Anal., **21** (199), pp. 799–818.

[25] V. Heuveline, R. Rannacher, *A posteriori error control for finite element approximations of elliptic eigenvalue problems*, J. Comput. Math. Appl., **15** (2001), pp. 107–138.

[26] J. Heywood, R. Rannacher, *Finite-element approximation of the nonstationary Navier–Stokes problem. I. Regularity of solutions and second-order error estimates for spatial discretization*, SIAM J. Numer. Anal., **25** (1982), pp. 275–311.

[27] P. Houston, E. Süli, *Adaptive Lagrange-Galerkin methods for unsteady convection-diffusion problems*, Math. Comp., **70** (2001), pp. 77–106.

[28] X. Hu, Y.-J. Lee, J. Xu, C.-S. Zhang, *On adaptive eulerian-lagrangian method for linear convection-diffusion problems*, J. Sci. Comput., **58**(2014), pp. 90–14.

[29] T. J. R. Huge, M. Mallet, A. Mizukami, *A new finite element formulation for computational fluid dynamics: II. Beyond SUPG*, Comput. Methods Appl. Mech. Engrg., **54** (1986), pp. 341–355.

[30] V. John, P. Knobloch, *On spurious osciallations at layers diminishing (SOLD) methods: Part I – A review*, Comput. Methods Appl. Mech. Engrg., **196** (2007), pp. 2197–2215.

[31] V. John, P. Knobloch, *Adaptive computation of parameters in stabilized methods for convection-diffusion problems*, in A. Cangiani et al. (eds.), *Numerical Mathematics and Advanced Applications 2011*, Springer, Heidelberg, 2013.

[32] V. John, J. Novo, *A robust SUPG norm a posteriori error estimator for stationary convection-diffusion equations*, Comput. Methods Appl. Mech. Engrg., **255** (2013), pp. 289–305.

[33] V. John, E. Schmeyer, *Finite element methods for time-dependent convection-diffusion-reaction equations with small diffusion*, Comput. Methods Appl. Mech. Engrg., **198** (2008), pp. 475–494.

[34] U. Köcher, M. Bause: Variational space-time methods for the wave equation, J. Sci. Comput., **61** (2014), pp. 424–453.

[35] U. Köcher: Variational Space-Time Methods for the Elastic Wave Equation and the Diffusion Equation, PhD Thesis, Helmut Schmidt University Hamburg, http://edoc.sub.uni-hamburg.de/hsu/volltexte/2015/3112/, 2015.

[36] D. Kuzmin, R. Löhner, S. Turek (eds.), *Flux-Corrected Transport: Principles, Algorithms, and Applications*, Springer, Berlin 2012.

[37] G. Lube, G. Rapin, *Residual-based stabilized higher-order FEM for advection-dominated problems*, Comput. Methods Appl. Mech. Engrg., **195**, (2006), pp. 4124–4138.

[38] D. Meidner, B. Vexler, *Adaptive space-time finite element methods for parabolic optimization problems*, SIAM J. Cobntrol Optim., **46** (2007), pp. 116–162.

[39] M. Picasso, V. Prachittham, *An adaptive algorithm for the Crank-Nicolson scheme applied to a time-dependent convection-diffusion problem*, J. Comput. Appl. Math., **233** (2009), pp. 1139–1154.

[40] A. Quarteroni, A. Valli, *Numerical Approximation of Partial Differential Equations*, Springer, Berlin, 2008.

[41] R. Rannacher, F. T. Suttmeier, *A posteriori error estimation and mesh adaptation for finite element models in elasto-plasticity*, Comput. Methods Appl. Mech. Engrg., **176** (1999), pp. 333-361.

[42] T. Richter, *Goal-oriented error estimation for fluid-structure interaction problems*, Comput. Methods Appl. Mech. Engrg., **223–224** (2012), pp. 28–42.

[43] T. Richter, T. Wick, *Variational localizations of the dual weighted residual estimator*, J. Comput. Appl. Math., **279** (2015), pp. 192–208.

[44] H.-G. Roos, M. Stynes, L. Tobiska, *Robust Numerical Methods for Singularly Perturbed Differential Equations*, Springer, Berlin, 2008.

[45] M. Schmich, B. Vexler, *Adaptivity with dynamic meshes for space-time finite ele-*

ment discretizations of parabolic equations, SIAM J. Sci. Comput., **30** (2008), pp. 369–393.

[46] K. Schwegler, *Adaptive goal–oriented error control for stabilized approximations of convection-dominated problems*, PhD Thesis, Helmut Schmidt University, http://edoc.sub.uni-hamburg.de/hsu/volltexte/2014/3086/, 2014.

[47] V. Thomée, *Galerkin Finite Element Methods for Parabolic Problems*, Springer, Berlin, 2006.

[48] R. Verfürth, *A posteriori error estimators for convection-diffusion equations*, Numer. Math., **80** (1998), pp. 641–663.

[49] R. Verfürth, *Robust a posteriori error estimates for stationary convection-diffusion equations*, SIAM J. Numer. Anal., **43** (2005), pp. 1766–1782.

[50] R. Verfürth, *Robust a posteriori error estimates for nonstationary convection-diffusion equations*, SIAM J. Numer. Anal., **43** (2005), pp. 1783–1802.

[51] R. Verfürth, *A Posteriori Error Estimation Techniques for Finite Element Methods*, Oxford University Press, Oxford, 2013.

A. Appendix

For the sake of completeness we provide the proof of Theorem 3.2.

Proof. We let $e = x_c - x_d$. By the fundamental theorem of calculus it holds that

$$\mathcal{L}(x_c) - \mathcal{L}(x_d) = \int_0^1 \mathcal{L}'(x_d + se)(e)\,\mathrm{d}s\,.$$

Approximating the integral by the trapezoidal rule yields that

$$\mathcal{L}(x_c) - \mathcal{L}(x_d) = \frac{1}{2}\mathcal{L}'(x_d)(x_c - x_d) + \frac{1}{2}\mathcal{L}'(x_c)(x_c - x_d) + \mathcal{R} \tag{A.1}$$

with $\mathcal{R}$ being defined by (3.20). By the supposed stationarity of $\mathcal{L}$ in x_c along with the assumption (3.18) the second of terms on the right-hand side of (A.1) vanishes. Together with eq. (3.17) we then get that

$$\begin{aligned}\mathcal{L}(x_c) - \mathcal{L}(x_d) &= \frac{1}{2}\mathcal{L}'(x_d)(x_c - y_d) + \frac{1}{2}\mathcal{L}'(x_d)(y_d - x_d) + \mathcal{R} \\ &= \frac{1}{2}\mathcal{L}'(x_d)(x_c - y_d) + \frac{1}{2}\mathcal{D}(x_d)(y_d - x_d) + \mathcal{R}\end{aligned}$$

for all $y_d \in X_d$. This completes the proof of Theorem 3.2. □